Bulletin of the Earthquake
Research Institute
University of Tokyo
Vol. 61 (1986) pp. 167-202

Report on DELP 1984 Cruises in the Middle Okinawa Trough
PART II: Seismic Structural Studies

Shozaburo NAGUMO[1], Hajimu KINOSHITA[2], Junzo KASAHARA[1], Toru OUCHI[3], Hidekazu TOKUYAMA[4], Toshio ASAMUMA[2], Sadayuki KORESAWA[1] and Hinako AKIYOSHI[2]

1) Earthquake Research Institute, University of Tokyo
2) Department of Earth Sciences, Chiba University
3) Department of Earth Sciences, Kobe University
4) Ocean Research Institute, University of Tokyo

(Received April 18, 1986)

Abstract

Multi-channel reflection records across the Central Rift Zone of the Middle Okinawa Trough, near the Natsushima-84 Deep in which an extremely high heat flow was observed, indicate reflections that are probably from the top of a magma chamber.

Refraction seismic study using 10 OBS's and four tons of explosives indicated that the crust of the Middle Okinawa Trough has a 5 km thick 6.0 km/sec layer above a highly attenuating 6.8 km/sec layer. Moho was not detected even at epicentral distances greater than 130 km. The crust was considered to be continental but low in Q in its lower part and the uppermost mantle to be anomalously low in both wave velocity and Q.

Observations of natural earthquakes, carried out for about one month by 10 OBS's, detected highly active micro-seismicity in the area. Some OBS's recorded particular phases which suspect of reflections from magma sheets as well as particular waves similar to volcanic tremors.

A. Multi-channel Seismic Profiles

The seismic structures of the topmost part of the surveyed area were studied by means of a multi-channel seismic profiling system through the KT-84-14 cruise of the TANSEI-MARU, the Ocean Research Institute, University of Tokyo. Three continuous track lines were planned in order to cross over a conspicuous depression (Iheya Deep) elongated along a NE-SW direction (Fig. II-1). One of the three lines (Line 2) crosses a graben, tentatively called Natsushima-84 Deep (see

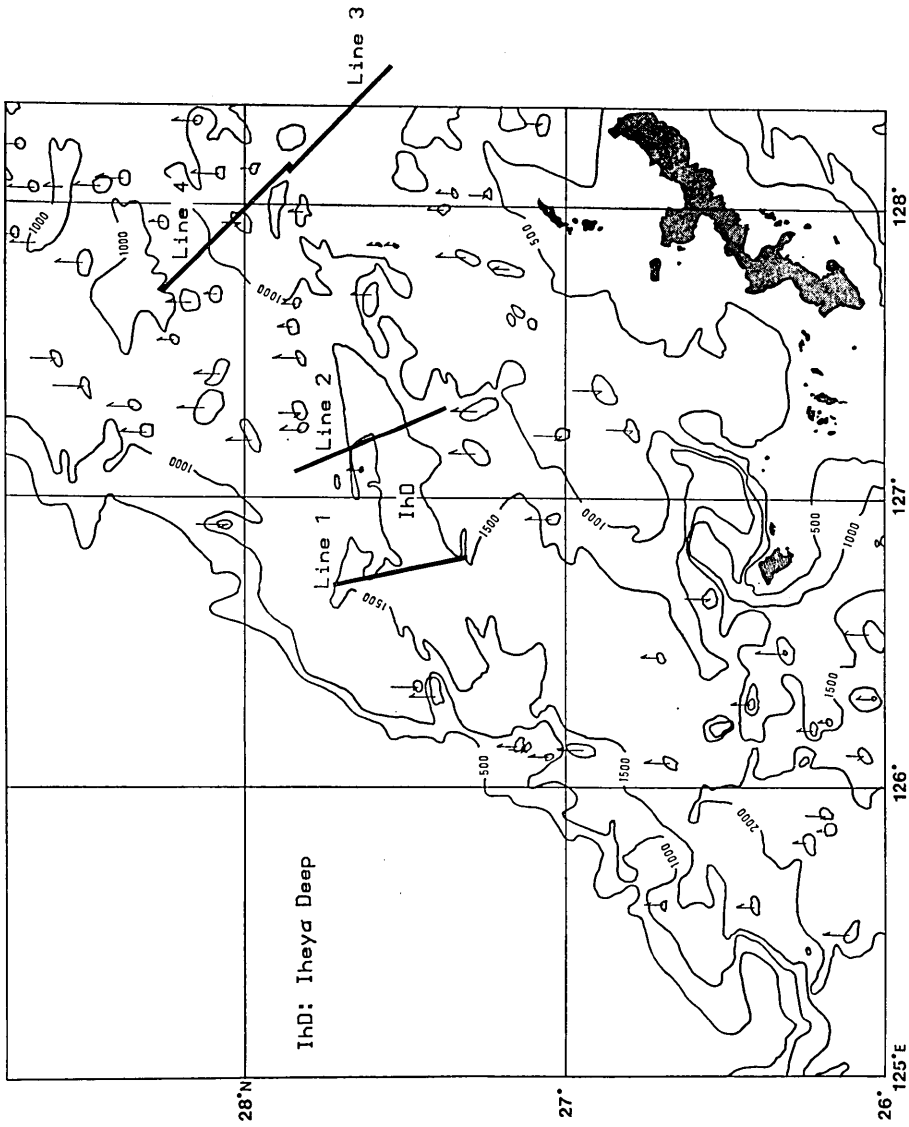

Fig. II-1. Track lines for multi-channel seismic profilers.

Table II-1. Some characteristic features of hydrophone streamer cable.

Section name	Length (m)	Number of elem.
Lead-in section	100	1
Weighted section	3	1
Stretch section	25	2
Dead section	25	2
Active section	50	6
Stretch section	25	1
Tail section	150	1
Depth/distance section	1	3

Depth in water; approx. 10 m
Distance between vessel and the ship side end of the active section; approx. 200 m

Characteristic features of airgun

Line No.	Volume of gun
1, 2	120 cubic inches (1.8 lit.)
3, 4	300 cubic inches (5.0 lit.)

Pressure of compressor; approx. 100 atm
Depth in water; approx. 10 m

Section V of this report) where a series of high heat flow values were obtained by two recent cruises (DELP-84 WAKASHIO, Part IV of this report and SONNE 34, YAMANO *et al.* 1986). The area was studied in detail in 1984 prior to the KT-84-14 cruise by use of seabeam mapping by R/V TAKUYO of Japan Maritime Safety Agency and R/V JEAN-CHARCOT and also through visual observations by the submersible Shinkai 2000 (UYEDA *et al.* 1985). Two other lines are running approximately parallel to Line 2 about 50 to 100 miles away. The seismic profiler data were processed by on-shore study through stacking, filtering and deconvolution to obtain better refined cross sections.

The multi-channel seismic profiler system is composed of a hydrophone streamer towed about 300 meters behind the vessel, a pneumatic airgun and an on-board digital data acquisition equipment. Some characteristic features of the system are listed in Table II-1. During the whole cruise, the airgun was shot every 20 seconds while the vessel was running straight with a steaming velocity of five knots which in turn means a shot every 50 meters.

Track lines of the seismic profiling study are shown in Fig. II-1. The northeastern line was divided into two sections and numbered as

Line 3 and 4 for convenience in the later data processing.

Cross sections of the seismic profiles after processing are shown in Figs. II-2 through II-5 where the vertical scale is expressed in two-way travel time, and the horizontal direction is aligned from left (SE end of lines) to right (NW end) with a thick bar representing a 10 km distance calculated from ship's positioning by the NNSS-incorporated Loran C navigation system. The profiles in Figs. II-2 through II-5 are provisionally interpreted as shown in Figs. II-6 through II-9 referring to the land geology of the Ryuku island arc (KIMURA 1985; UJIIE 1985). The continuous thick sedimentary basement layer (Layers A and B) in the surveyed area could be correlated to the Shimajiri Formation composed of a pile of soft muddy materials and probably formed in the late Miocene (6 Ma–7 Ma) to early Pleistocene. However, there seems to be no layers

Table II-2. Positions of track lines of multi-channel seismic profiles.

L. No.	(Start at)		(End at)		Track Line Length (km)
	Lat.	Long.	Lat.	Long.	
1	27-43.4	126-41.3	27-17.86	126-46.91	47.95
2	27-22.2	127-19.3	27-50.7	127-04.7	56.8
3	27-38.1	128-25.4	27-52.40	128-06.83	39.7
4	28-10.3	127-46.8	27-51.40	128-08.5	51.45

Table II-3. Interpretation of seismic profiles.

Line 1 (Fig. II-6)

The stratigraphic sequence is classified into three units. By correlating the seismic sequence with the data from test drill wells TO-KA-1 and OKINAWA 1x, we interpret the upper two units (A and B) as the Shimajiri Formation from late Miocene to Pleistocene and the lowest unit (C) as Cretaceous strata.

Many normal faults appear in the lowest unit indicating that block movements occurred by tensional stress.

An active normal fault appears in the middle part of the profile covered by thick sediment.

Line 2 (Fig. II-7)

The Shimajiri Formation appears on both ends of the profile but it is scarcely visible in the middle part. Topographic rises seem to be intrusive igneous rock bodies.

Many normal faults are observed in the lowest unit similar to Line 1. Active normal faults appear in the middle part as observed in other pull-apart basins.

Possible reflections from the roof of a magma chamber are detected beneath the central rift.

Line 3 (Fig. II-8)

The Shimajiri Formation is barely visible.

Line 4 (Fig. II-9)

Active normal faults appear on both ends.

The lowest unit forms a large graben shaped depression and thick sediment covers it.

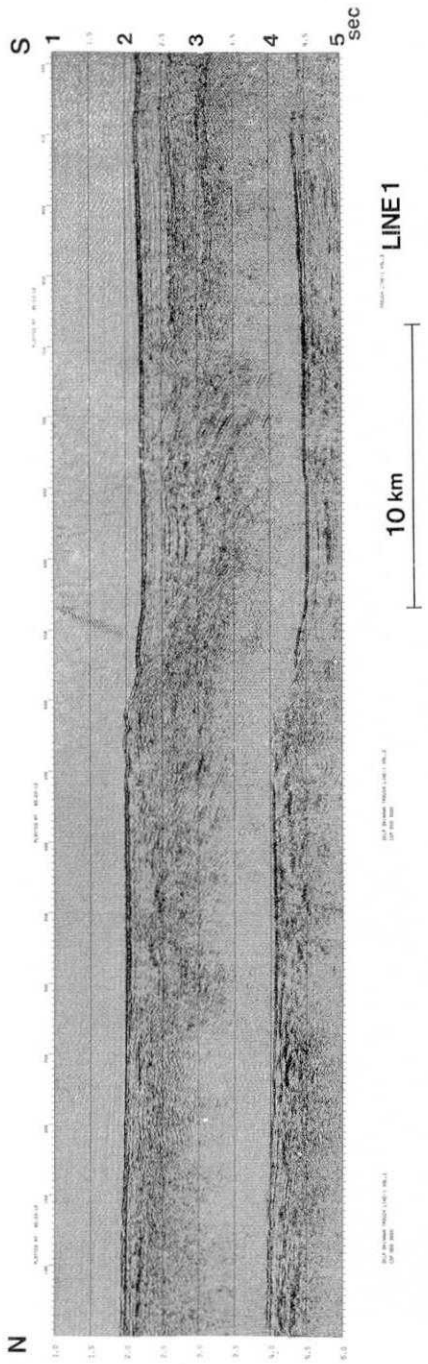

Fig. II-2. Refined seismic profile of Line 1.

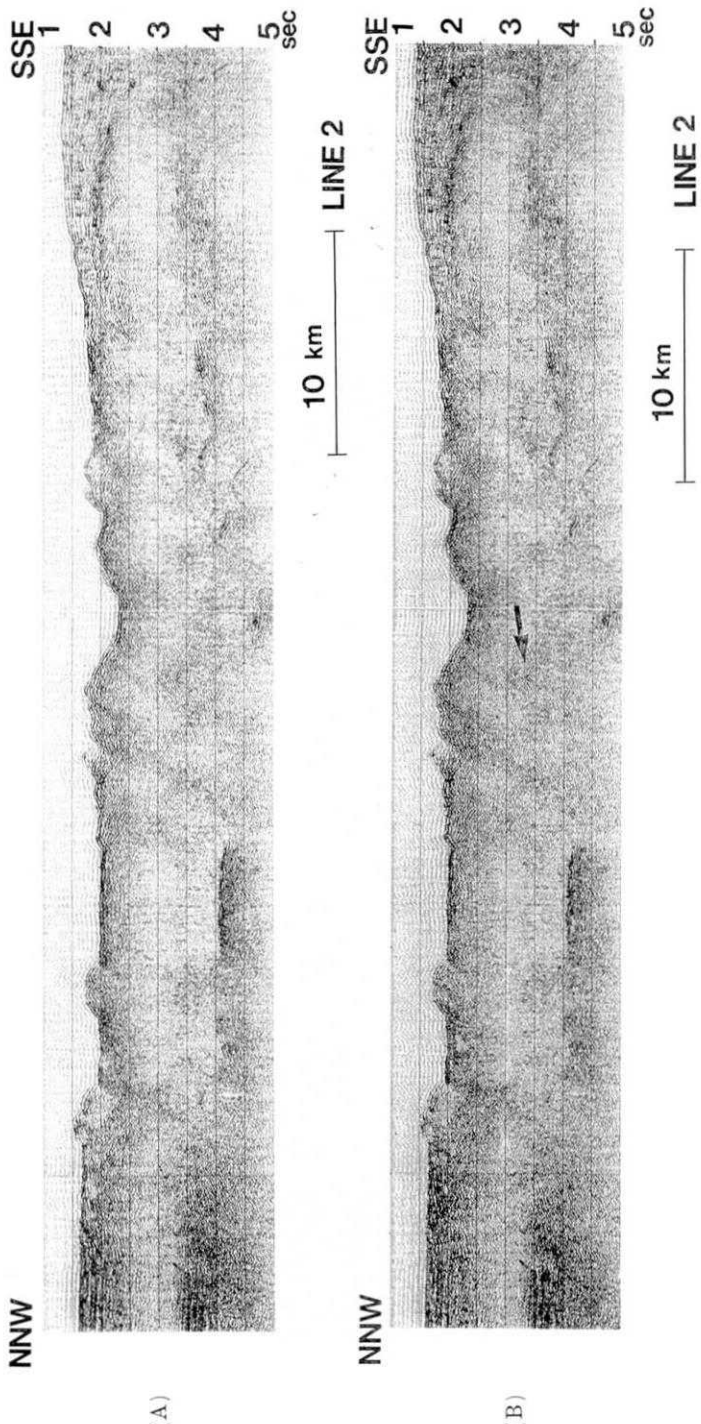

Fig. II-3. (A) Refined seismic profile of Line 2.
(B) The same as (A) but high constrast showing vague reflectors in the central rift (arrow mark).

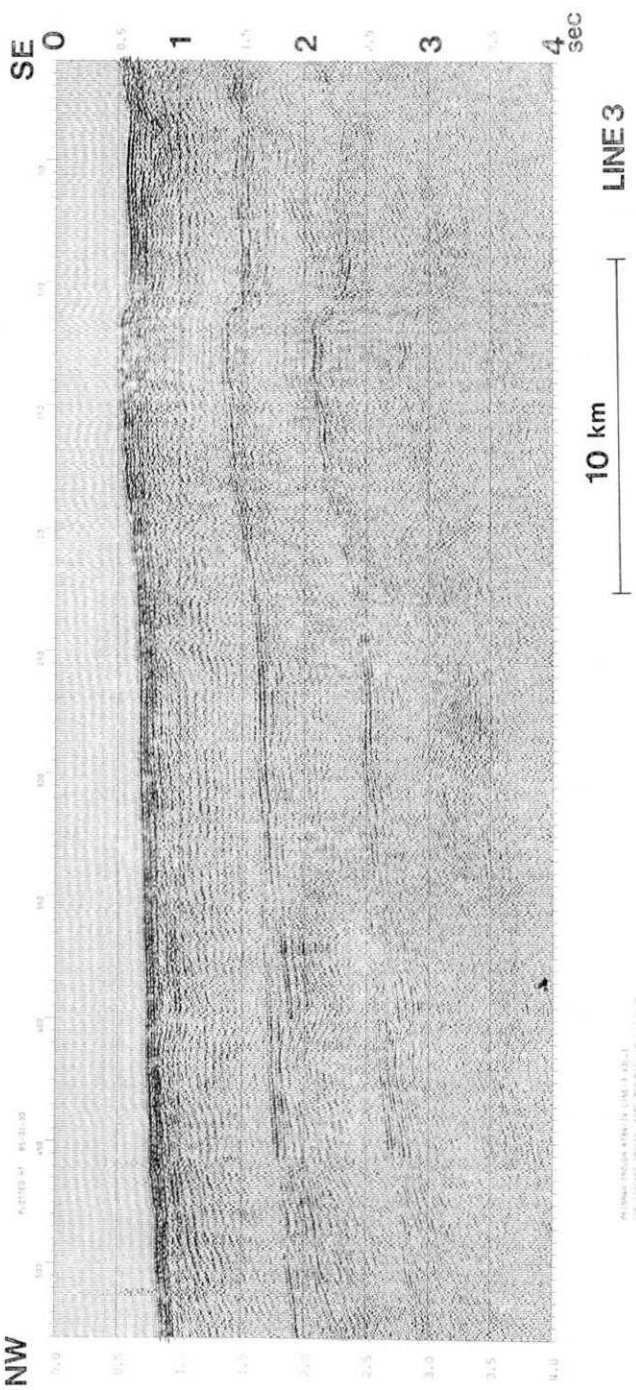

Fig. II-4. Refined seismic profile of Line 3.

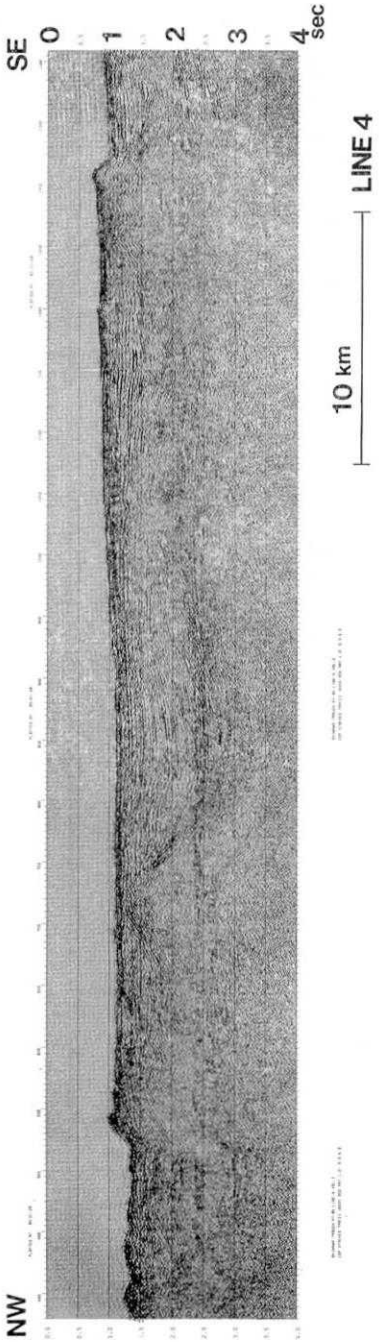

Fig. II-5. Refined seismic profile of Line 4.

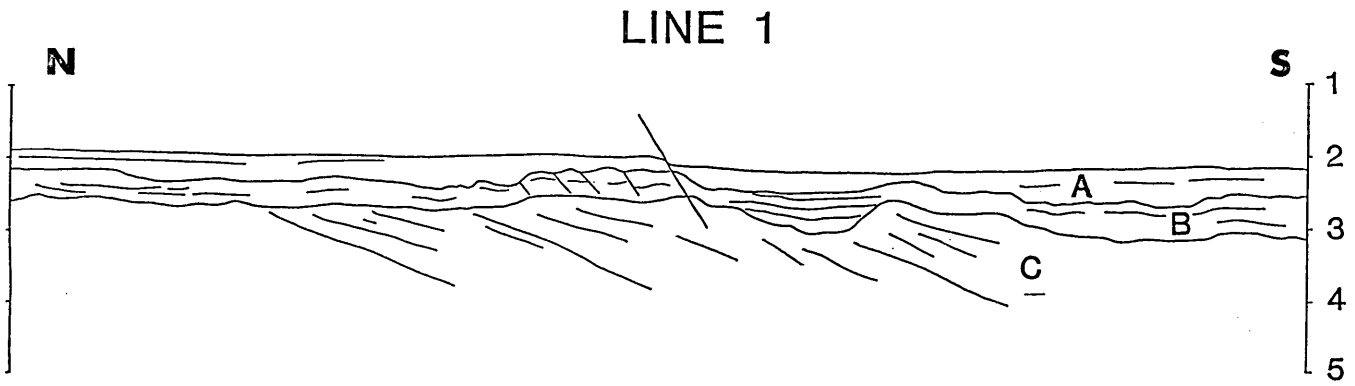

Fig. II-6. Interpretations of seismic profile, Line 1.

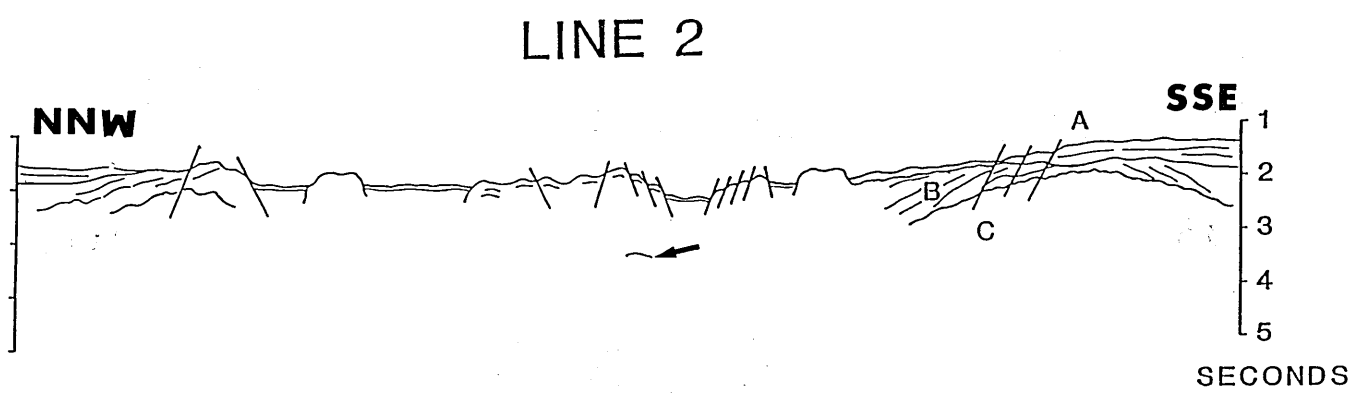

Fig. II-7. Interpretations of seismic profile, Line 2. An arrow mark: vague reflector from a probable magma chamber where a phase inversion of wave packet was studied.

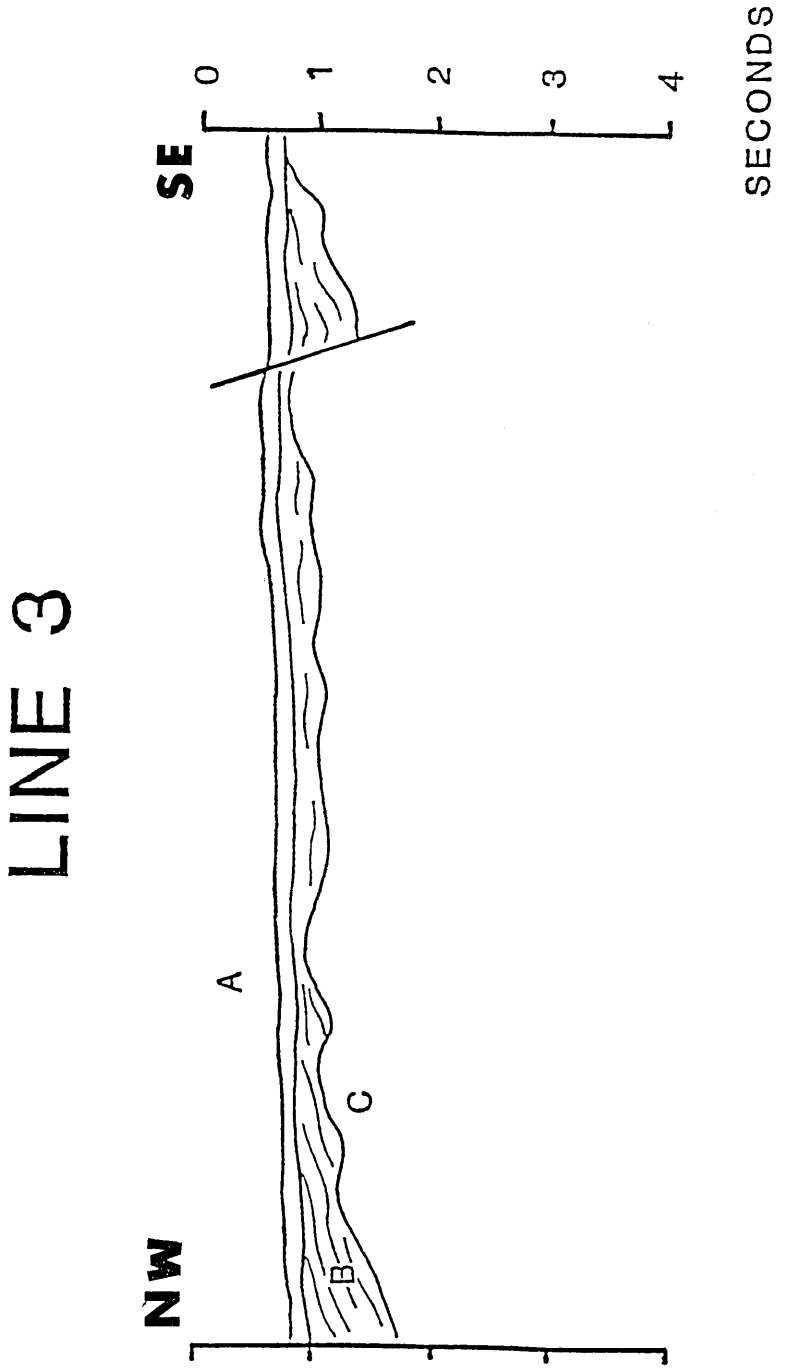

Fig. II-8. Interpretations of seismic profile, Line 3.

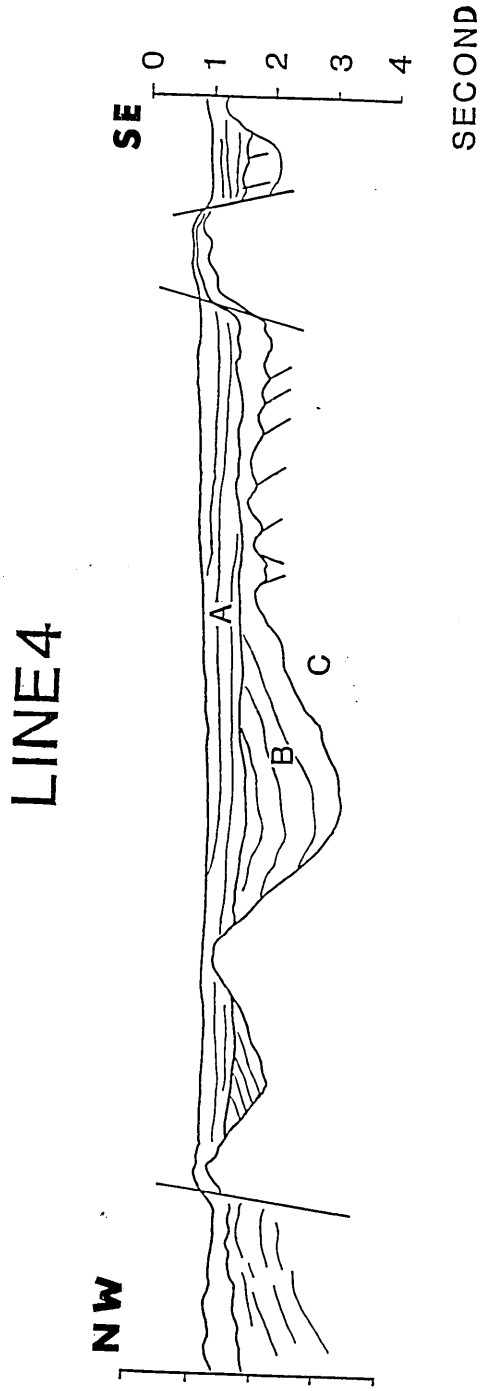

Fig. II-9. Interpretations of seismic profile, Line 4.

A pnd B in the narrow central part of Line 2 (Natsushima-84 Deep in the Iheya Deep where extremely high heat flow values were observed). This portion shows a structure which is very similar to the typical structure of crustal rifting as seen on the on-board monitoring rocords (Figs. II-10 through II-13). The graben (Iheya Deep) seems to be elongated in the NE-SW direction as revealed by seabeam mapping.

Characteristic internal structures of the formation inferred from these four seismic records are briefly summarized in Table II-3.

In addition to the conventional profiling study, variations of reflection waveforms were examined in the central part of the presumed rift along Line 2. It was found that a wave packet of the shooting wave reverses its phase at around the depth where a vague reflector (arrow in Fig. II-3B and II-7) can be traced in the central rift. If there is a good

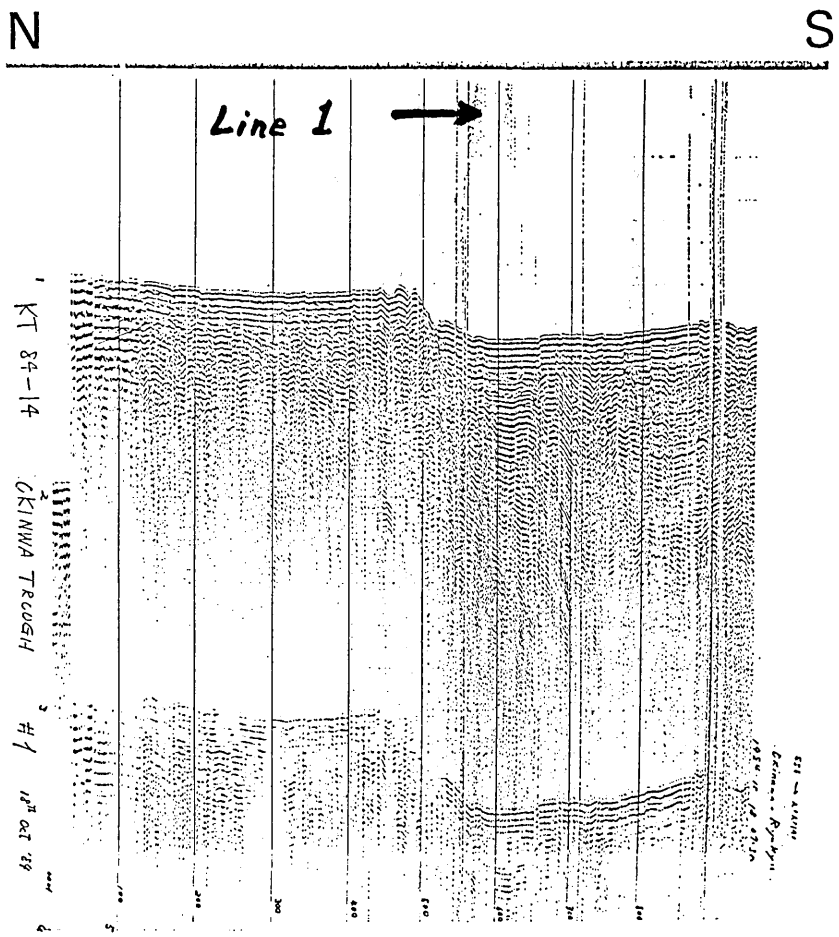

Fig. II-10. On board monitor records of single channel seismic profiler, Line 1.

method to subtract or eliminate multi-reflection ghost patterns in the profiler records, this vague feature could be more precisely traced. Elimination of the multi-reflection phase is being attempted at present with more refinement of data. At the present stage, however, it may be said that the vague boundary mentioned above carries a characteristic feature of an interface between hard rock (upper layer) and soft materials (lower) or at least of a very high downward negative gradient in velocity structure. Even though the evidence on the multi-channel seismic profile itself is not sufficiently convincing, this boundary may correspond to the interface between rock cover and a magma chamber when the surprisingly high heat flow values (1500 mW/m^2, Section IV of this report) are taken in account. This problem is also discussed later in the section C where the results of deep structural study by explosion shooting, combined with ocean bottom seismometer observation, are presented.

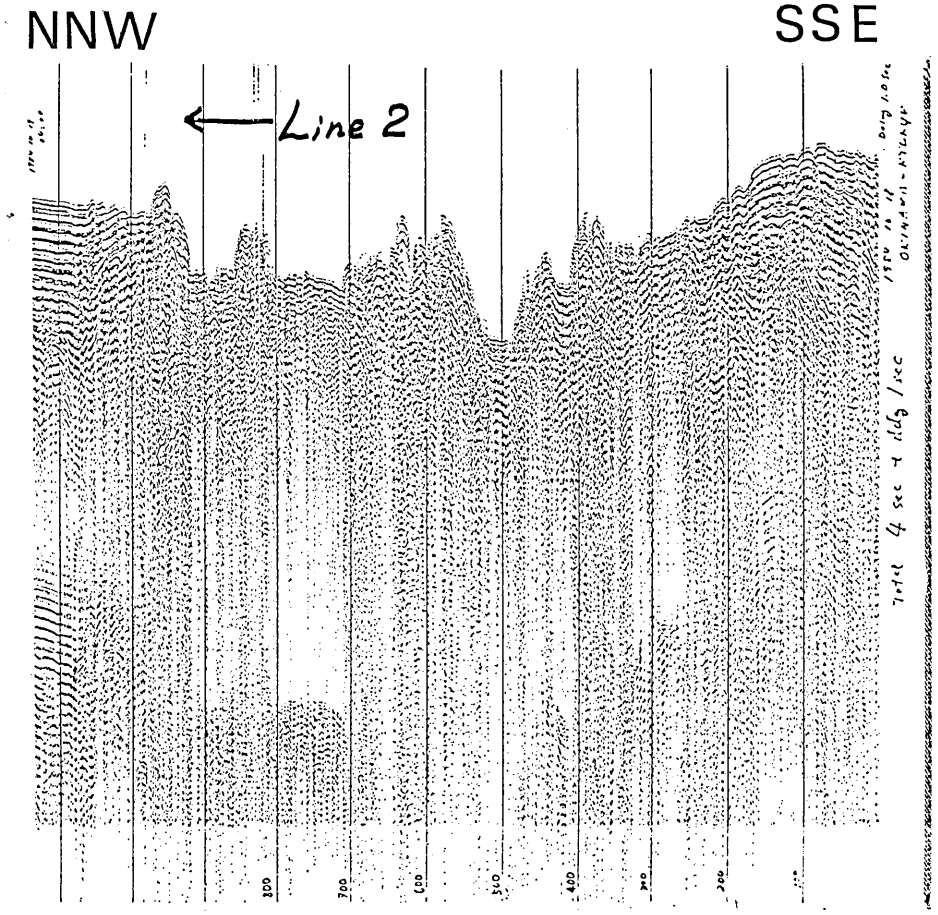

Fig. II-11. On board monitor records of single channel seismic profiler, Line 2.

B. Airgun—OBS operations for the study of fine crustal structure

Airgun shooting was used for clarifying the fine crustal structures by means of the refraction method. Two long lines of airgun shooting and the area of explosion shooting are covered by 10 sets of OBS as shown in Fig. II-14. One of the 10 OBS's is a digital OBS developed by

Table II-4. Location and water depth of OBS's.

OBS. No.	Deployment Date	Lat.	Long.	W.D. (m)
OK- 1	1984.08.25	26-39.16	126-06.00	1928
OK- 2	1984.08.25	27-07.69	126-39.79	1853
OK- 3	1984.08.26	27-35.98	127-13.09	1467
OK- 4	1984.08.26	27-29.65	126-43.59	1689
OK- 5	1984.08.25	27-27.93	126-38.46	1634
OK- 6	1984.08.26	27-40.79	127-29.11	1469
OK- 7	1984.08.25	26-30.88	125-48.98	1686
OK- 8	1984.08.25	26-20.09	126-02.54	2074
OK- 9	1984.08.26	27-41.99	126-41.67	1484
OK-10	1984.08.25	26-40.90	126-30.61	1710
OK-11	1984.09.02	27-19.24	127-21.67	1255

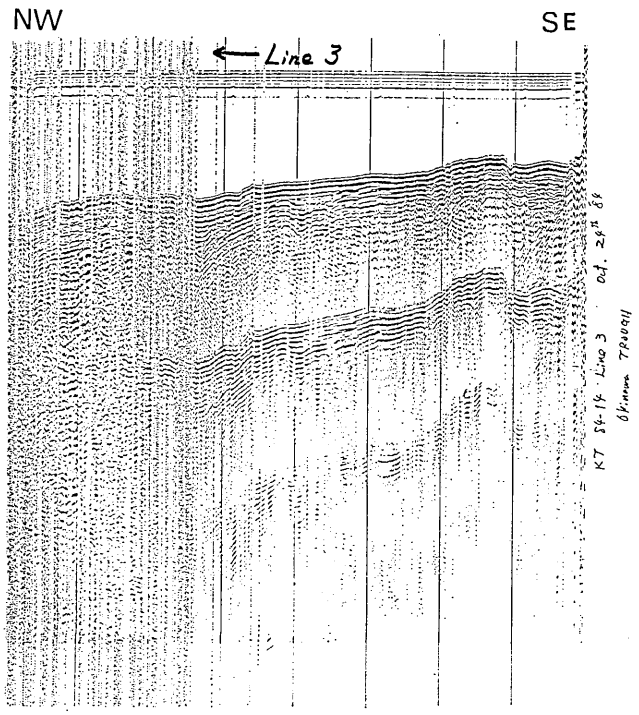

Fig. II-12. On board monitor records of single channel seismic profiler, Line 3.

KASAHARA *et al.* (1985) and was deployed to test its seabottom performance. The location and water depth (W.D. in meters) of all the OBS's are listed in Table II-4.

Bathymetric cross sections along Lines A and B (Fig. II-14) are shown in Figs. II-15 and 16. Two pairs of OBS's (Nos. 2 and 3, and Nos. 4, and 6) were to be used for airgun-OBS structural study. However, it was found after all the OBS's were recovered that No. 4 was not running for unknown reason. The positions of the other OBS's (No. 2, 3 and 6) are also shown on the bathymetric records in Figs. II-15 and 16.

The physical and mechanical features of the airgun are listed in Table II-5. The shooting interval could hardly be controlled precisely because the triggering of the blast could be obtained only by balancing pressures between the blast and confining chambers. The shooting instances, therefore, were picked up through an acoustic element located close to the airgun chamber towed behind the vessel. The blast sound was sent to the vessel through electric wire and a set of digital timer

Table II-5. Pneumatic Airgun (large volume)

Volume; 10 liter
Pressure; 100 atm
Shooting interval; ca. 180 sec.

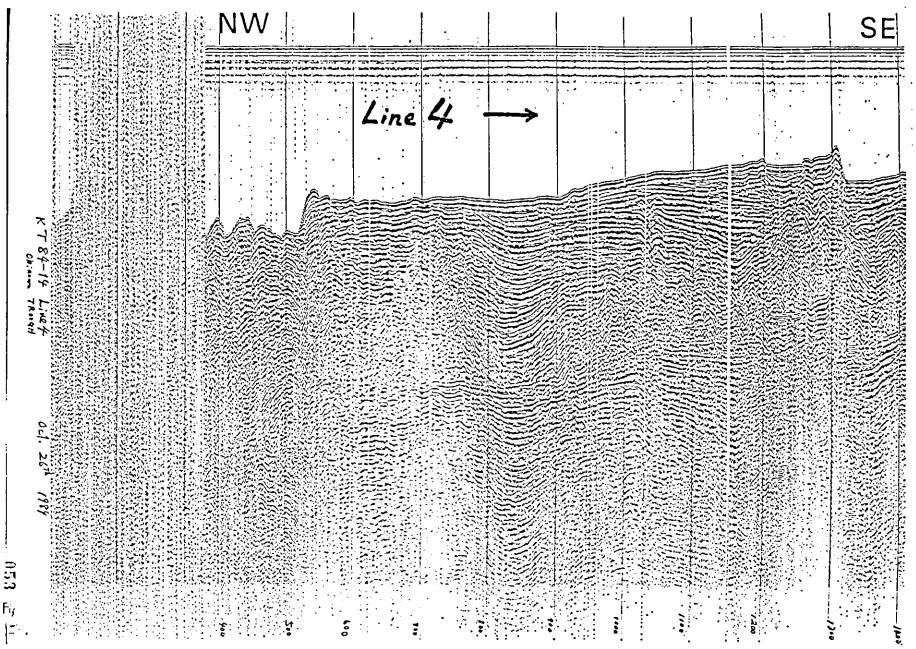

Fig. II-13. On board monitor records of single channel seismic profiler, Line 4.

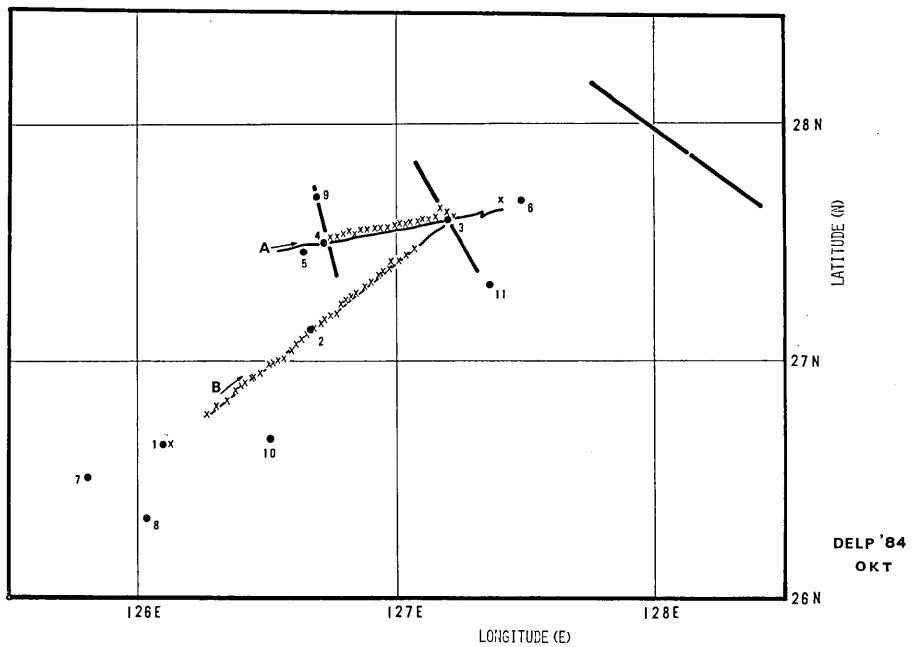

Fig. II-14. Location of seismic refraction lines (A and B with arrows), multi-channel seismic survey lines (NW-SE trending thick bars), Ocean Bottom Seismometer and Hydrophone stations (OBSH; solid circles with station numbers) and shot points of dynamite explosions (thin crosses). Unit of coordinates: degree.

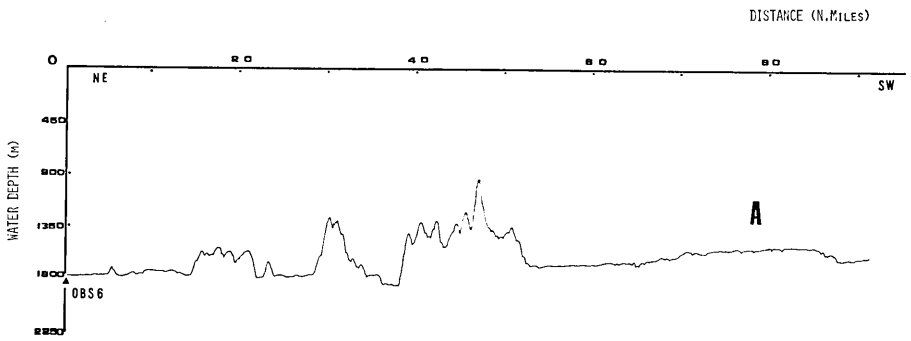

Fig. II-15. Bathymetric features along survey line A as referred in Fig. II-14. Distances are given in relation to station No. 6 toward SWW along survey line A in units of nautical miles for convenience of data analyses. Water depths are given in units of meters.

devices was activated by the sound pulse to provide digital shot instance data. Shot instances of the airgun were corrected to the Japan Standard Time (JJY). Airgun shooting dates were from July 30, $14^{H}57^{M}$ to July 31, $06^{H}21^{M}$ (453 shots) for Line A, and from Aug. 1, $08^{H}24^{M}$ to Aug. 1,

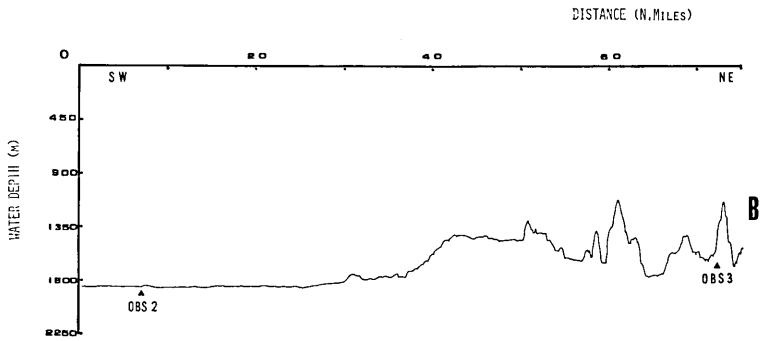

Fig. II-16. Bathymetric features along survey line B in the proximity of the OBS stations 2 and 3 from the SW side toward the NE side. Further details are referred to in a caption of Fig. II-15.

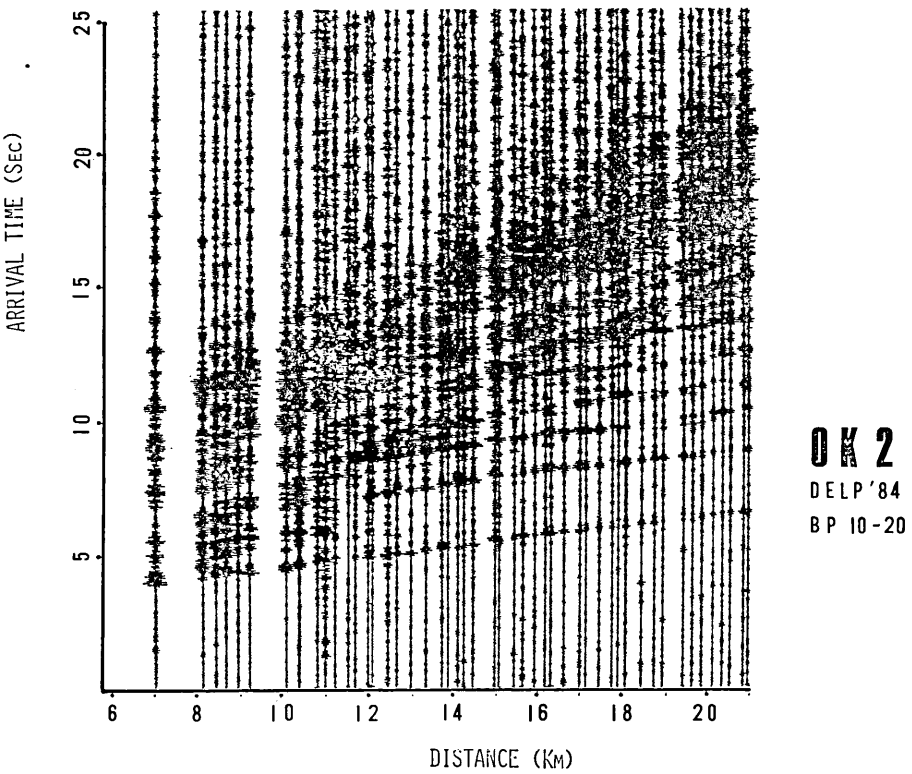

Fig. II-17. An example of distance-time section display on way of the seismic structural analyses. Data are shown from OBSH records (output from Hydrophone) obtained at station 2 (OK-2). Filter: band-pass, 10-20 Hz with stop frequency 30 Hz.

$20^{H}59^{M}$ (339 shots) for Line B. (The list of the corrected shot time data are available from the authors.)

Analog data of the OBS's were then digitized and a series of editing measures were applied to the original wave records. The distance between OBS and the sound source was calculated by using the arrival time of the water break combined with the water depths of the OBS. After all these editing procedures, the time-distance sections of the filtered wave record were displayed on a high speed laser printer connected to computer systems.

An example of the computer output of the filtered band-pass phase which is used to determine the distance of OBS-airgun pair is shown in Fig. II-17. After obtaining the time-distance record section, more steps of data processing have to be applied to reconstruct the fine structure of the surveyed area. A simple horizontal layering model (shown in Fig. II-18) gives only a crude velocity structure around the three terminal points of Lines A and B.

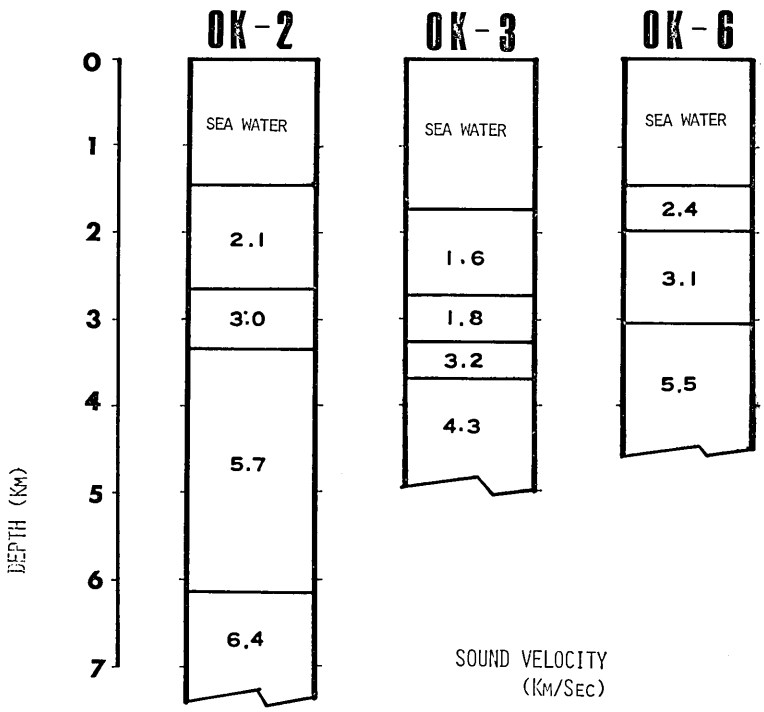

Fig. II-18. Crude seismic crustal structures obtained by a series of airgun refraction studies by OBSH at stations OK-2, OK-3 and OK-6. Depths from the sea surface are shown in units of km along a vertical line on the left. Values in the columns are seismic velocities in units of km/sec.

C. Explosion seismic refraction survey

1. Introduction

The objectives of the explosion seismic refraction survey in the Middle Okinawa Trough of the DELP-84 WAKASHIO cruise were two-

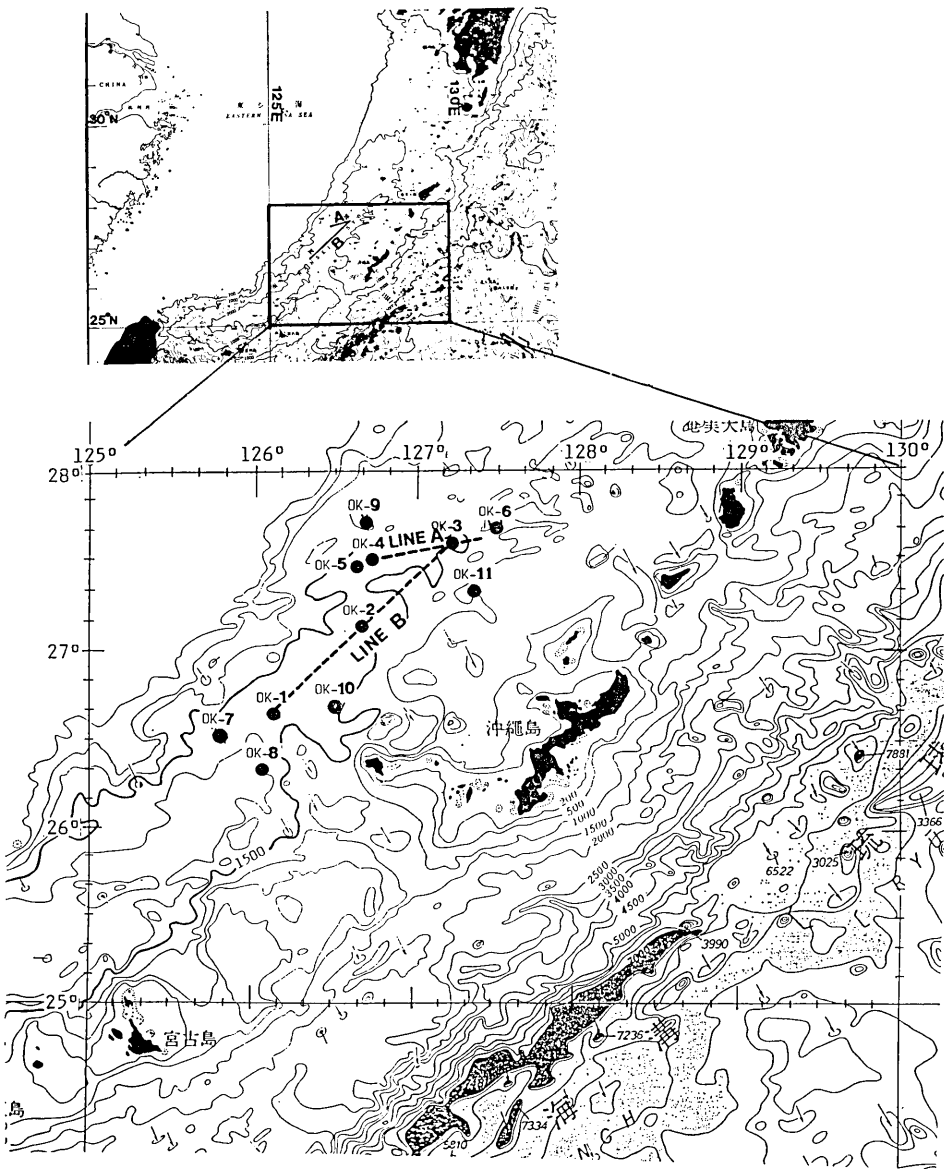

Fig. II-19. Location of seismic refraction survey Line A and Line B. Solid circle: OBS stations (OK-1～OK-11).

fold: firstly, to see if any oceanic crust has already been formed beneath the trough axis and secondly, when the oceanic crust has not yet been formed, to see how far the continental crust has been destroyed. Several mechanisms have been proposed for the back-arc basin formation, for instance, stretching, thinning, necking, spreading, rifting, oceanization, collapse, faulting and fragmentation etc.

We expect the seismic data to tell us which of these are actually taking place in the Middle Okinawa Trough. Topographically, the Middle Okinawa Trough tends to terminate towards the northeast. The water depths in the axial zone are shallower (about 2200–2500 m) than those in the Southwestern Okinawa Trough, where the existence of an ocean crust has been reported (LEE *et al.* 1980). Therefore the Middle Okinawa Trough was considered to be a suitable place to study the mechanism and process of the initiation of the back-arc basin formation.

2. Outline of the experiment

We performed two shooting lines: Line A, right above a segment

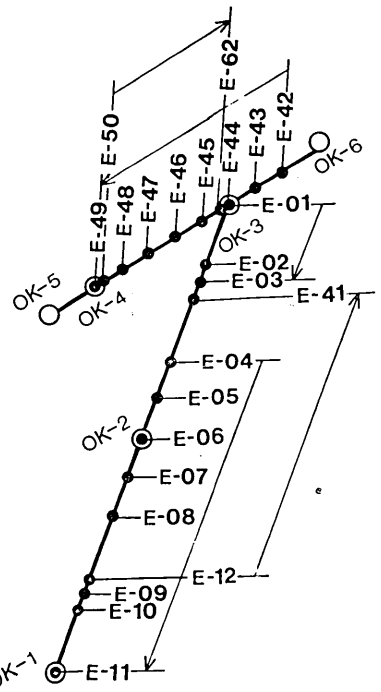

Fig. II-20. Configuration of shot points and OBS stations.
Line A: Shots E-42~E-62 for OBS stations OK-6 and OK-5.
Line B: Shots E-01~E-41 for OBS stations OK-1~OK-3.

of probable rift axis (Iheya Deep) and Line B, along the regional axial zone of the trough (Fig. II-19). We deployed 6 OBS's on these lines; namely, stations OK-5, 4, 3 and 6 on Line A, and stations OK-1, 2, 3, and 6 on Line B. In addition to these stations, we deployed another 5 OBS's (stations OK-7, 8, 9, 10 and 11) in the same area for the seismicity study as shown in Fig. II-19. These OBS stations also formed a configuration of fan-shooting. The OBS station data are given in Table II-4, and the explosion data (shot position, shot time, charge amount, water depth, ship speed etc.) are given in the Appendix. Explosives were dropped from the moving ship and detonated at the depth of about 100 m from the sea surface using fuse wire. Larger shots (125-500 kg) were fired at several points for detecting the Moho, and many small shots (2-50 kg) were fired at close intervals (2-20 km) for detecting shallow strata. The total amount of explosives was four tons, and the total number of shots was 64. The configuration of shot-point numbers and OBS stations is shown in Fig. II-20. The digital OBSH (at station OK-5) was recovered right after the shooting operation. The other OBS's

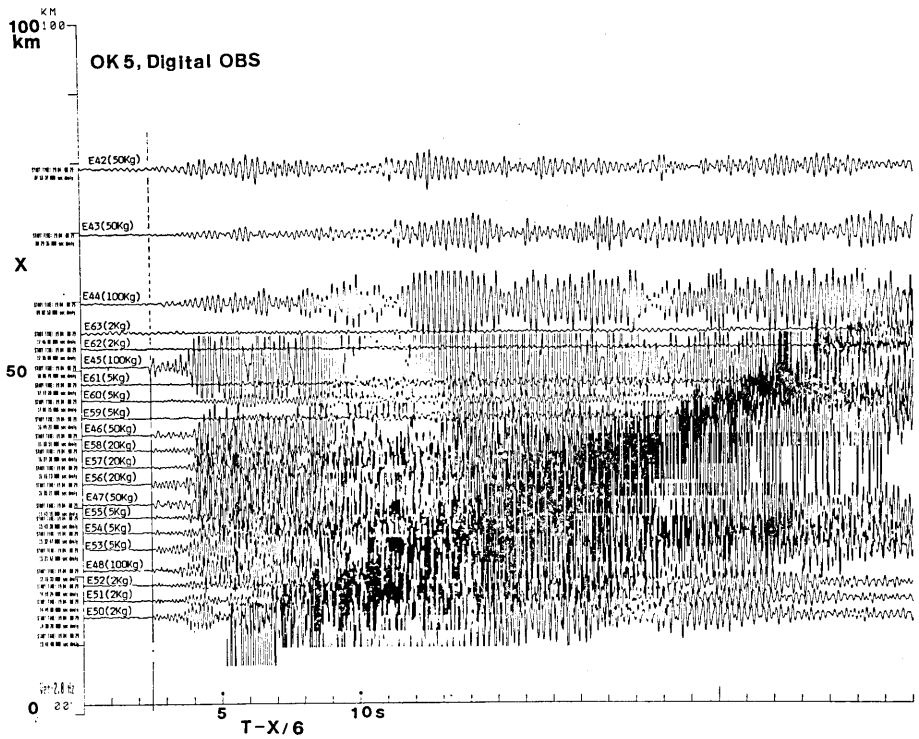

Fig. II-21. Record section (vertical component) for station OK-5 along Line A (Digital OBSH). Travel times are reduced by 6.0 km/sec.

were recovered during the cruise of the R/V TANSEI-MARU (KT-84-14) in October about two months after the shooting operation. This enabled us to record natural earthquakes for a period of about one month.

3. Instrumentation

We used 10 acoustic-release, free-fall-pop-up type OBS's, and one

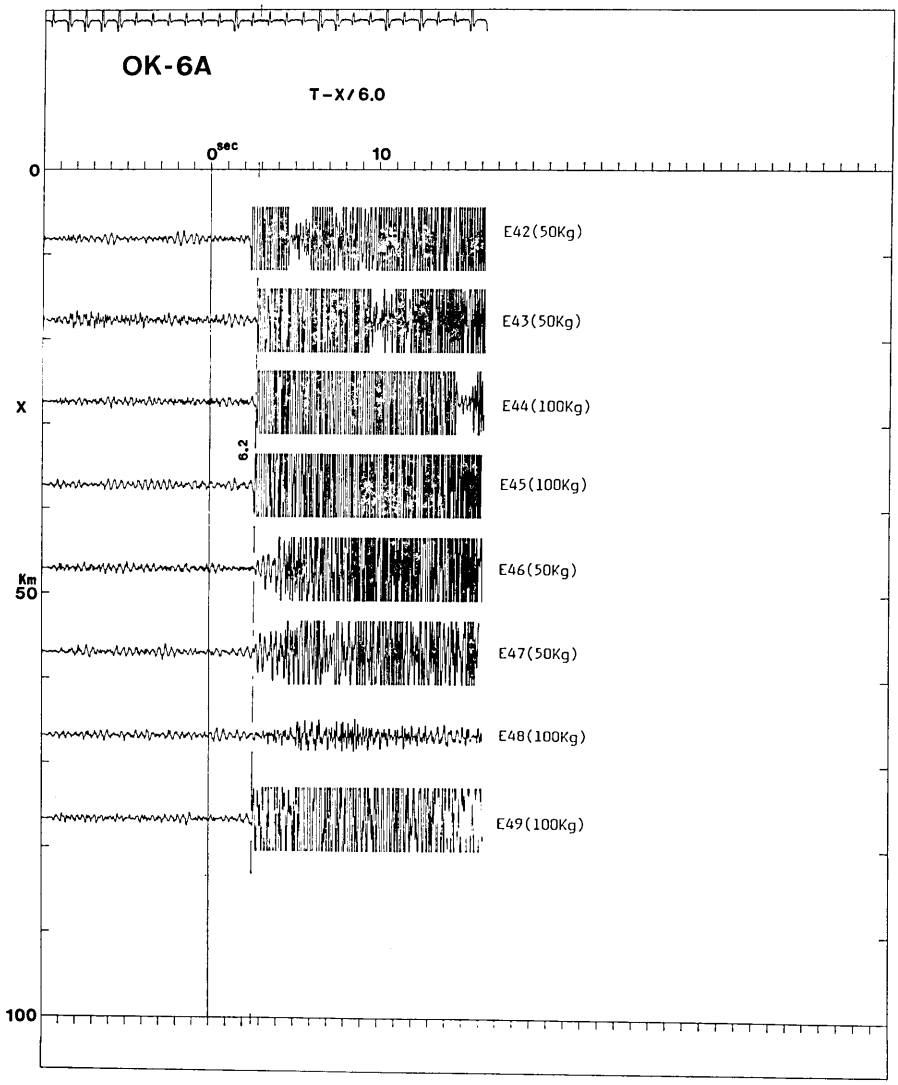

Fig. II-22. Record section (vertical component) for station OK-6 along Line A. Reduced velocity: 6 km/sec.

Digital OBSH, which has been recently developed (KASAHARA *et al.*, 1985). Since the operation area is in the route of the Kuroshio-Current, we omitted the use of the radio-beacon so as to escape the antenna noise which would be caused by a possible strong bottom current. The recovery operations were made by acoustic ranging. All the OBS's were recovered. For ship positioning, we used Loran-C combined with NNSS. The predetermined shot positions were occupied with high accurracy (less

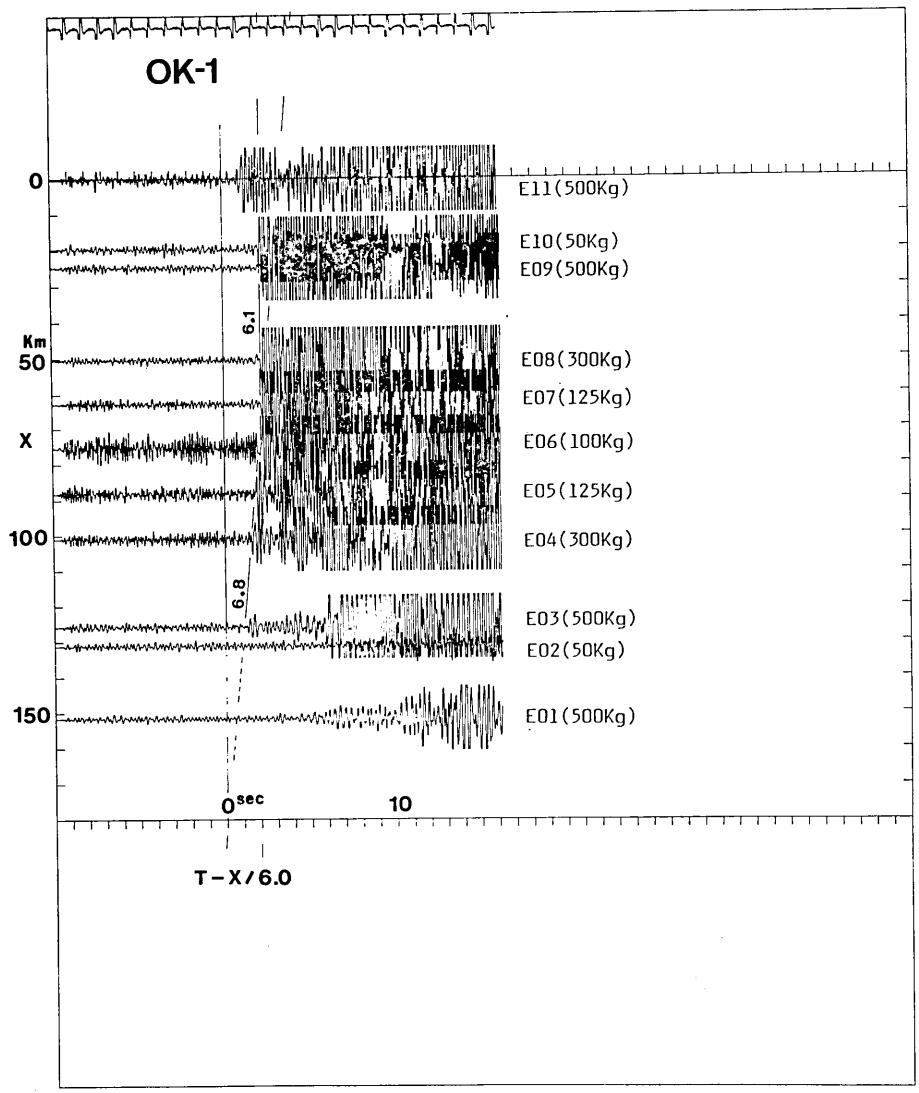

Fig. II-23. Record section (vertical component) for station OK-1 along Line B. Reduced velocity: 6 km/sec.

than 0.1 n. miles) by the navigation control using a real time ship-track display system.

4. Results

The travel-time record sections have been prepared. On these sections, we can directly see several important features of the crustal structure.

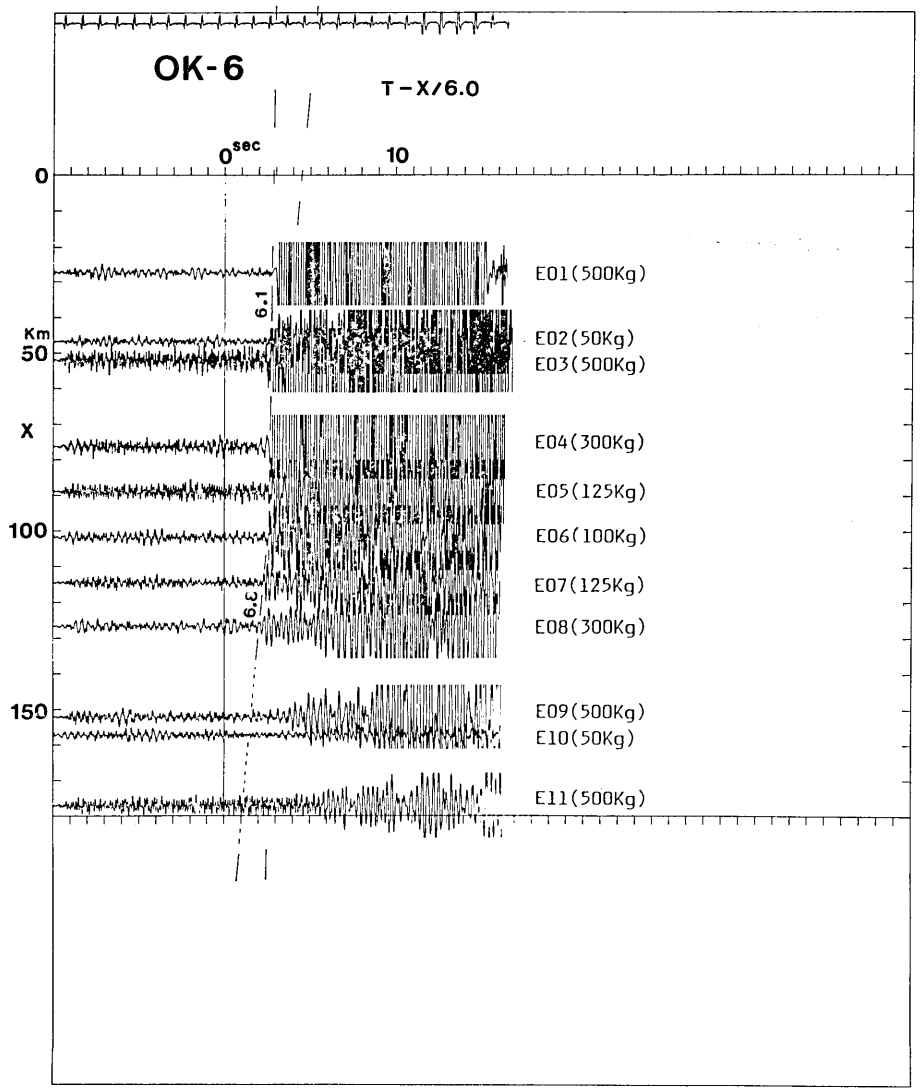

Fig. II-24. Record section (vertical component) for station OK-6 along Line B. Reduced velocity: 6.0 km/sec.

Line A: Along Line A, the sedimentary layer is underlain by a 6.0 km/s layer whose refractions appear as first breaks from the epicentral distance 20 km up to about 80 km for station OK-6, and up to 50 km for station OK-5. The travel-time record sections of Line A from station OK-5 and OK-6 are shown in Figs. II-21 and II-22 The 6.0 km/s layer could be a granitic layer, which is abundant in the neighbouring regions. Since Line A is selected along a segment of possible rift axis inferred

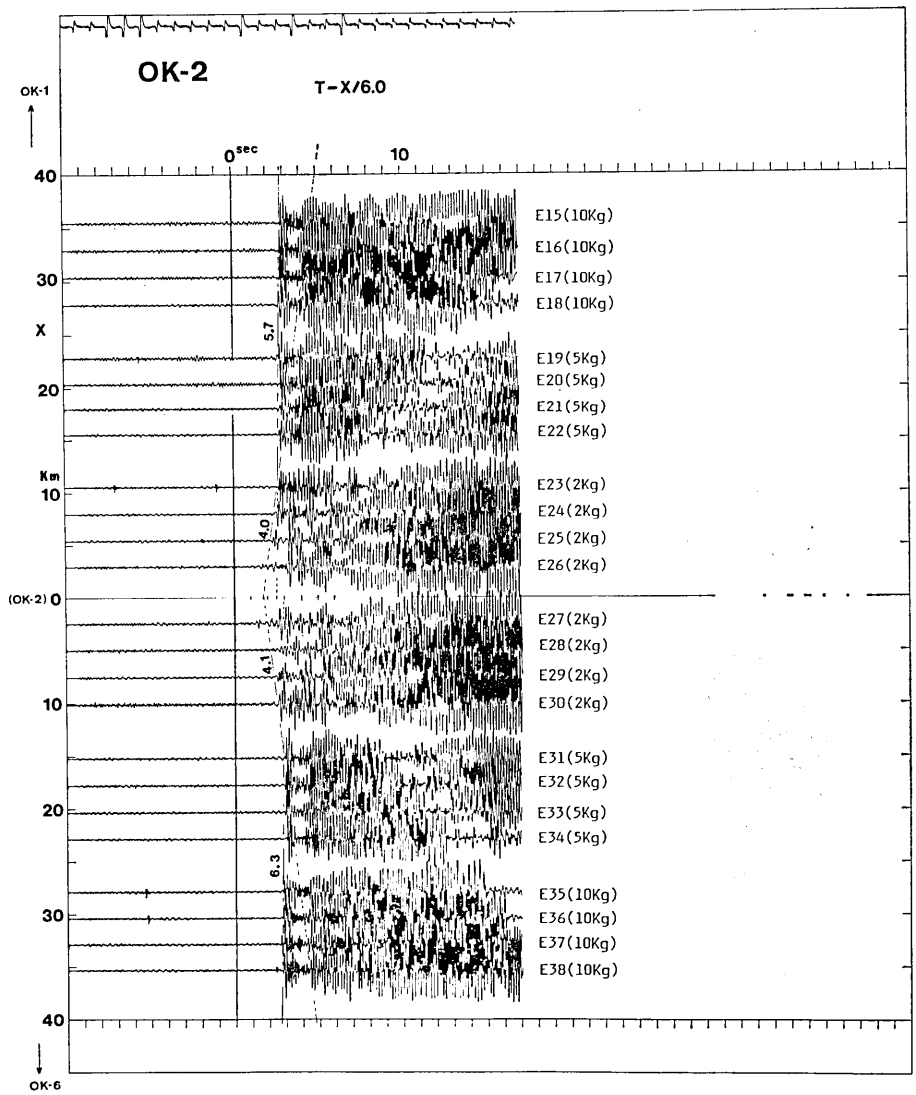

Fig. II-25. Record section (vertical component) for station OK-2 along Line B. Reduced velocity: 6.0 km/sec.

from topography (Part V of this report) and since is very close to an axial ridge (bathymetric map by R/V JEAN-CHRCOT cruise, 1984), it is likely that an oceanic crust has not yet been formed beneath the rift axis.

Line B: Along Line B, the 6.0 km/s layer is underlain by a 6.8 km/s layer, whose refractions appear as first breaks beyond the distance of about 70 km showing a cross-over of the travel time curves of 6.0 km/s and 6.8 km/s. The record sections of Line B from stations OK-1 and OK-6 are shown in Figs. II-23 and II-24. The attenuation of the 6.8 km/s refractions is remarkable and refractions diminish beyond the distance of about 130 km. No Moho refractions were detected over a 130 km distance in spite of the 500 kg charges. These features may indicate that the lower crust has been partially destroyed and the uppermost mantle beneath the axial zone is anomalous, probably low-velocity and also low-Q. The destruction might be caused not only by mechanical fracturing but also by thermal anelasticity as well as partial melting. At station OK-2, the sedimentary layer which overlies the 6.0 km/s layer has a velocity of 4.1 km/s, which is seen as first breaks up to a distance of about 10 km (Fig. II-25).

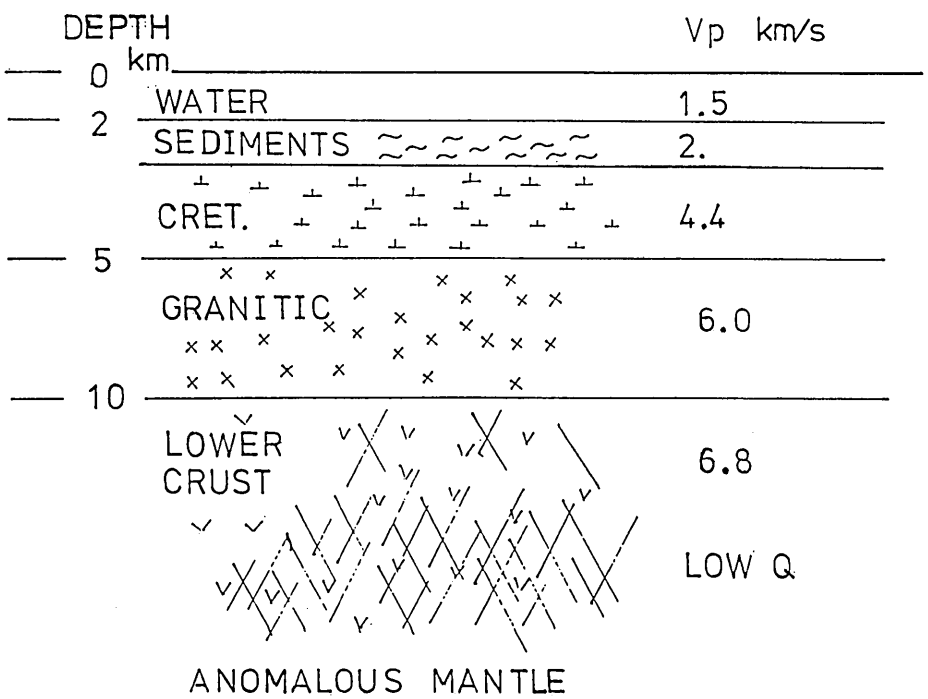

Fig. II-26. Approximate P-wave velocity structure in the Middle Okinawa Trough.

From the geological data of the area and multi-channel seismic reflection profiles in the adjacent area (section A of this Part II), the 4.1 km/s layer could be correlated with Cretaceous formations. The thickness of the 4.1 km/s layer may vary from station to station. In Fig. II-26 is shown an approximate structure of the layer-thickness and depth based on a calculation for the constant-velocity layered model.

5. Conclusion

The operation of the seismic refraction survey was very smooth and successful. We have obtained a considerable amount of good quality data. They can be used as a basis for further studies. The data presented in this report show that, under the Middle Okinawa Trough, there still remains a continental crust in which, however, destruction appears

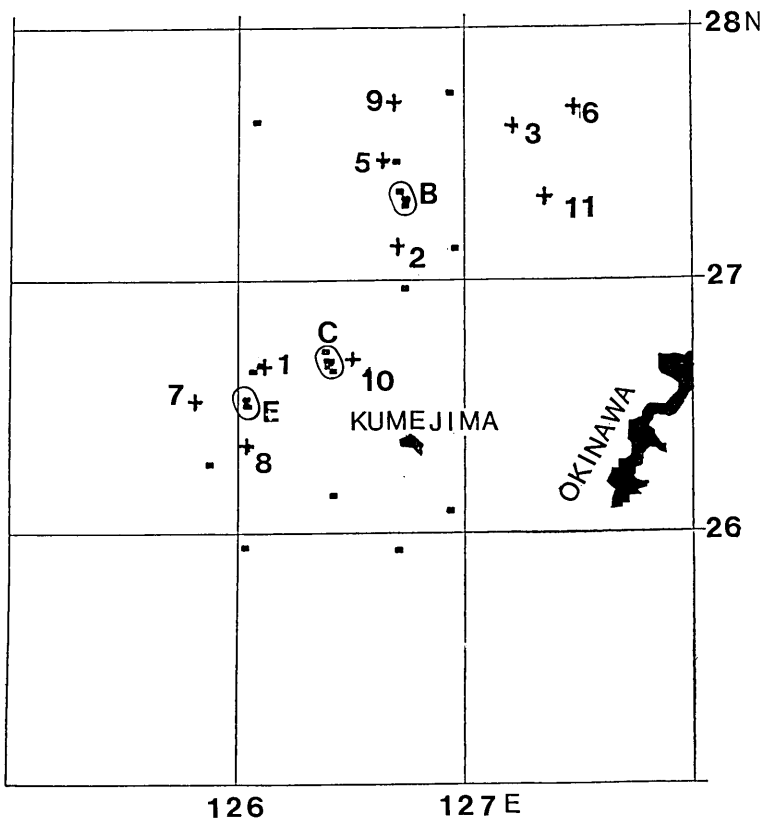

Fig. II-27. Distribution of hypocenters (mark ■) which are well determined by several OBS stations (mark +) during a period of about one month observation (July—August, 1984). The depths are shallow (less than 15 km). Three earthquake swarms are identified at the locations B, C and E (marked by circles).

to have reached its lower part and the uppermost mantle may be anomalously low in both velocity and Q.

D. Seismicity Studies

In order to study the natural earthquake activity in the region of the Middle Okinawa Trough, a network observation was made at the 10 OBS stations described in the preceding section C (Fig. II-19). We obtained a data-set of continuous good quality recordings for a period of one month from Aug. 26 to Sept. 26, 1984, at 8 stations (shown in Fig. II-27 and Table II-4). Although no micro-earthquake activity has been reported by landbased stations for a long period of time including our observation period, our OBS observation revealed intensive seismic activities in almost the whole region of the Middle Okinawa Trough. At almost all the

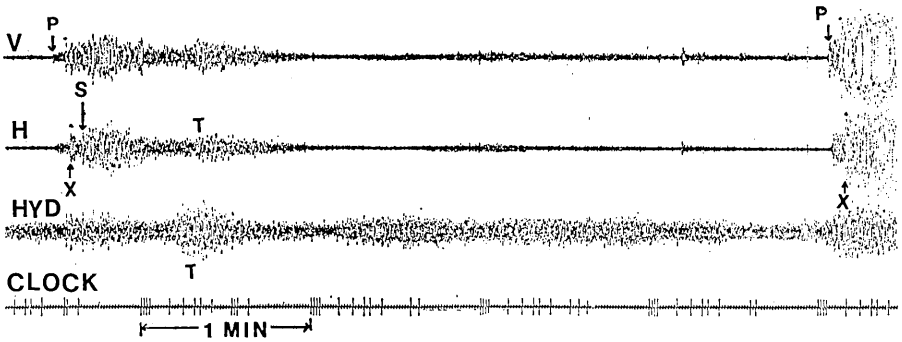

Fg. II-28. An example of peculiar phase x which appears between P and S phases, observed at the station OK-2. This may be a reflection from a possible magma sheet.

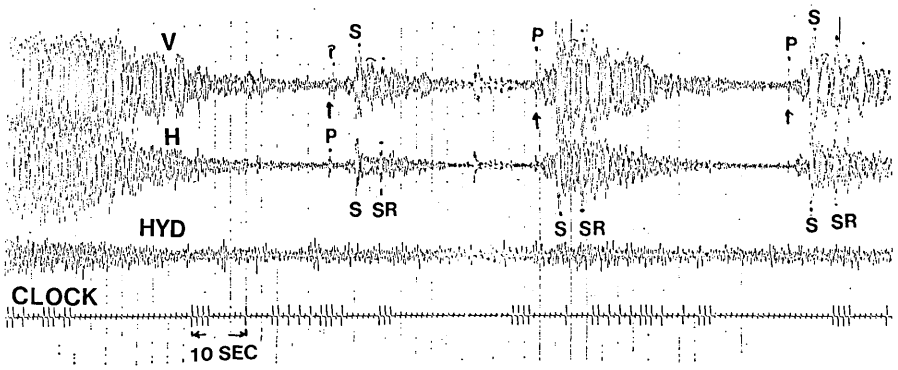

Fig. II-29. An example of another peculiar phase 'SR', which appear after S-arrivals, observed at station OK-2. This may be a reflection from a magma sheet.

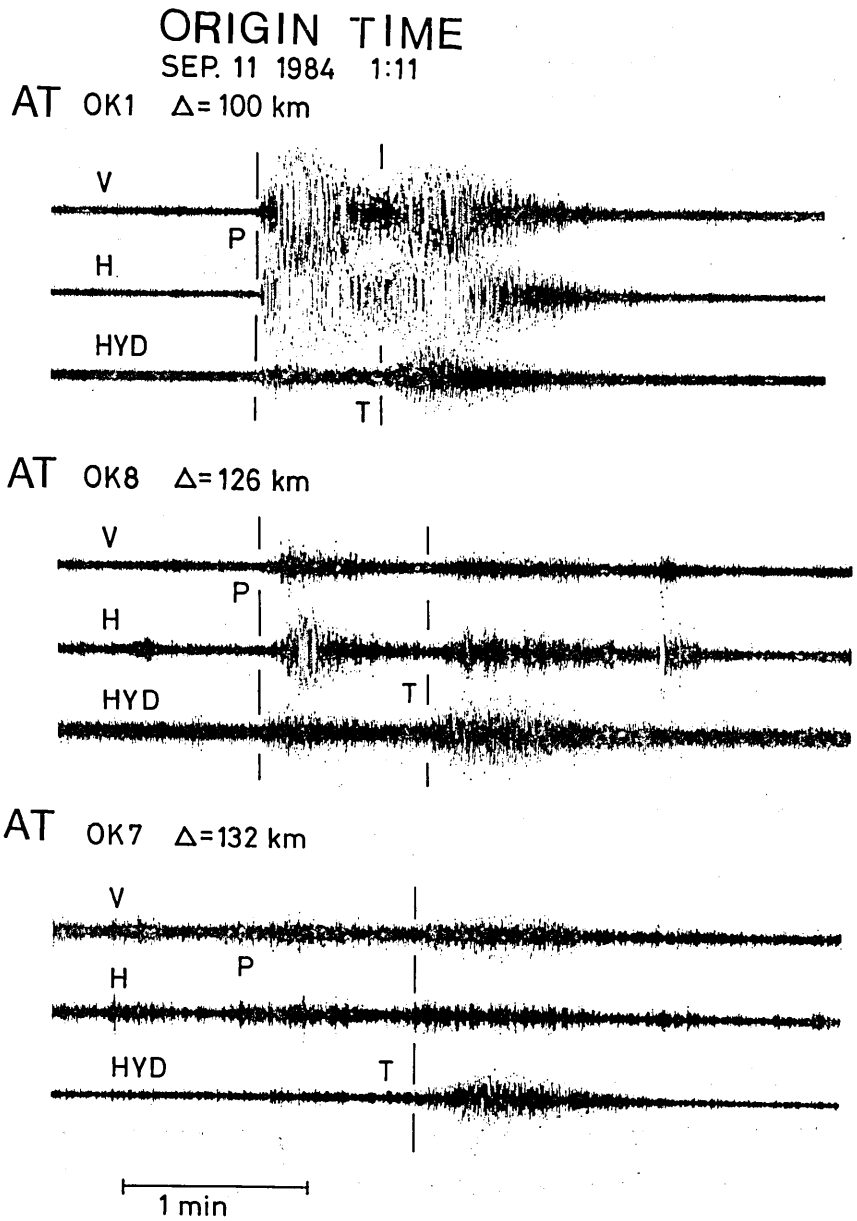

Fig. II-30. An example of attenuation of seismic waves beyond the epicentral distance of about 120 km. Records are at three station OK-1 (distance=100 km), OK-8 (distance=126 km) and OK-7 (distance=132 km). The epicenter and ray paths are shown in Fig. II-31. V: vertical component, H: horizontal component, HYD: hydrophone, P: arrival of P-phase, T: T-phase.

stations, micro-earthquake activities were recorded including several swarm earthquakes. Among them, at three stations (OK-2, OK-1 and OK-10), nearly 1000 micro-earthquakes were detected during a period of one month observation. The foci of a limited number of relatively large events among these swarm earthquakes were located at three places (Fig. II-27). One place was located between stations OK-5 and OK-2 (location B), near the western termination of the segment of the rift axis (seismic refraction Line A). The other two places were located near the axial zone of the trough; one between stations OK-10 and OK-1 (location C) and

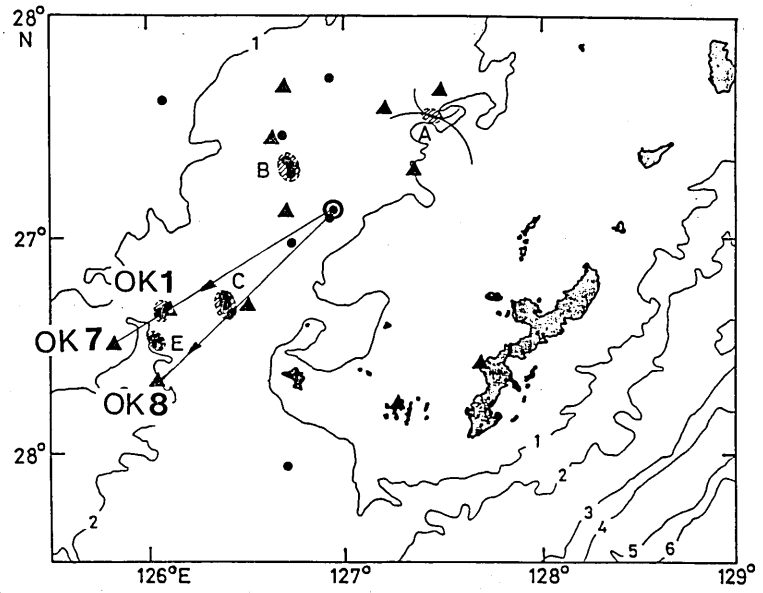

Fig. II-31. The ray paths for the records shown in Fig. II-30. The Epicenter (mark ⊙) is west of the station OK-2.

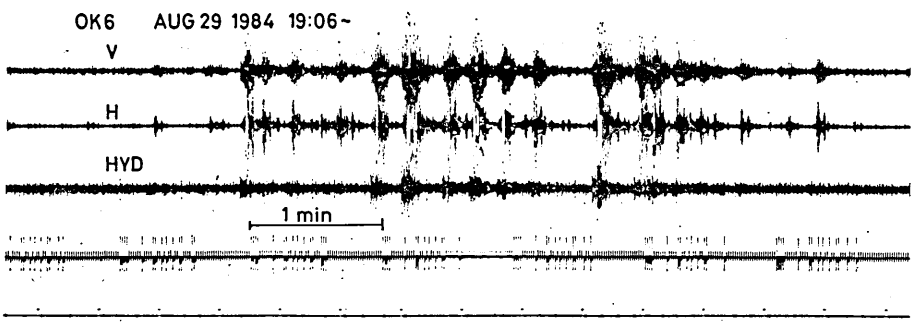

Fig. II-32. An example of earthquake swarm observed at station OK-6.

another slightly south of station OK-1 (location E). Interestingly, the sizes of these swarm earthquakes were nearly the same, being about M=3 or less.

Another interesting phenomenon to note was the the presence of peculiar phases on the earthquake seismograms. One was a phase appearing between P and S-phases, an example of which is shown (by a mark X) in Fig. II-28. This may be the converted phase either from P to S or S to P from some reflector which might exist along the ray path. The other was a phase appearing in later phases of S-phase, an example of which is shown (by a mark SR) in Fig. II-29. This may be the reflection of S-phase from some reflector. These phases indicate the presence of efficient reflectors which may be magma sheets.

Attenuation of seismic waves was large beyond the epicentral distance of about 120 km. An example is shown in Figs. II-30 and 31. This was consistent with the results obtained by the seismic explosion experiment.

Two kinds of signals, which closely resemble volcanic tremors were observed. One was a ceaseless occurrence of numerous isolated shocks

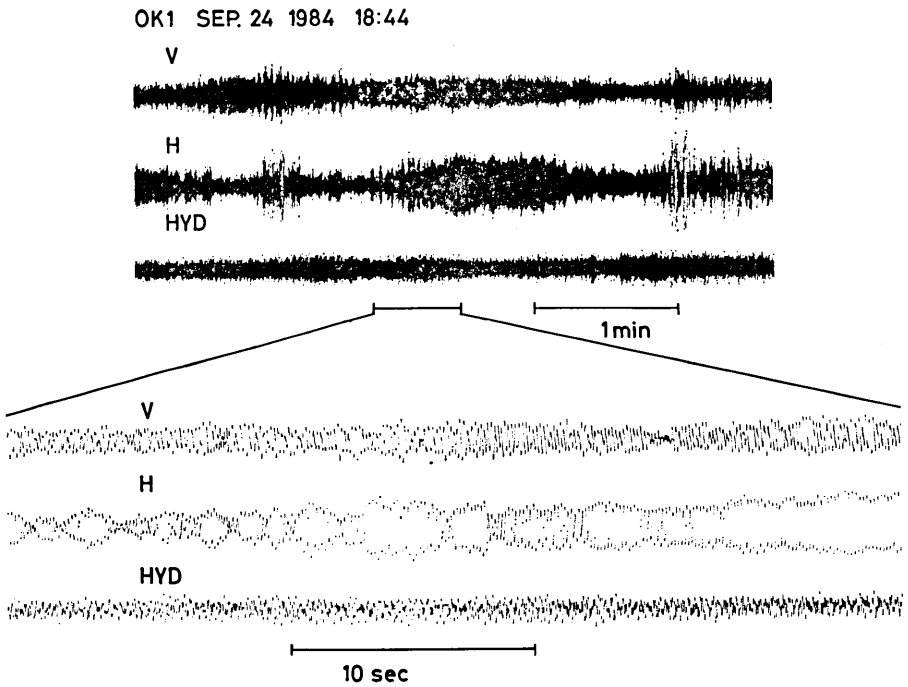

Fig. II-33. An example of records which suggests volcanic tremors observed at station OK-1.

(Fig. II-32). The other was a sinusoidal oscillation with predominant frequencies of 5-7 Hz (Fig. II-33).

These seismic features, when combined with the results of the seismic refraction study, indicate that the Middle Okinawa Trough has been subjected to an incipient spreading where the destruction of continental crust has reached the lower crust with magmatic activity.

References

KIMURA, M., 1985, Back-arc rifting in the Okinawa Trough, *Marine and Petroleum Geology*, **2**, 222-240.

LEE, C. S., G. G. SHOR, L. D. BIBEE, R. S. LU and T. W. C. HILDE, 1980, Okinawa Trough: Origin of a back-arc basin, *Marine Geology*, **35**, 219-241.

KASAHARA, J., M. TAKAHASHI, T. MATSUBARA and M. KOMIYA, 1985, Mass Storage Digital Ocean Bottom Seismometer and Hydrophone (DOBSH) Controlled by Micro-processors using ADPCM Voice Synthesizing, *Bull. Earthq. Res. Inst., Univ. Tokyo*, **60**, 23-37.

MURAUCHI, S., N. DEN, S. ASANO, H. HOTTA, T. YOSHII, T. ASANUMA, K. HAGIWARA, K. ICHIKAWA, T. SATO, W. J. LUDWIG, J. T. EWING, N. T. EDGER and R. E. HOUTZ, 1968, Crustal structure of the Philippine Sea, *J. Geophys. Res.*, **73**, 3143-3171.

UJIIE, H., 1985, A Standard Late Cenozoic Micro-biostatigraphy, *Bull. of the National Science Museum*, **11**, no. 3, 103-136.

UYEDA, S., N. KIMURA, T. TANAKA, I. KANEOKA, Y. KATO and I. KUSHIRO, 1985, Spreading Center of the Okinawa Trough, JAMSTECTR DEEPSEA RES., Sp. Pap., 123-142 (in Japanese with English abstract).

YAMANO, M., S. UYEDA, Y. FURUKAWA and G. A. DEHGHANI, 1986, Heat flow measurements in the Northern and Middle Ryukyu Arc area on R/V SONNE in 1984, *Bull. Earthq. Res. Inst., Univ. Tokyo*, **61**, 311-327.

Appendix

Explosion shot data: shot position (degree and minute), water depth (km), ship speed (kt), burning time (sec), change size (kg), and corrected shot time (JST). The correction of shot time is made to the sea-surface shot. The sinking speed of the explosive is 80 m/min. The shot depth was kept at 100 m from the sea-surface for shots whose sizes are larger than 100 kg.

Appendix Table 1.

LINE B

SHOT NO.	NAME	LAT D M N	LON D M E	DEPTH <M	DAY SHOT TIME1 D H M S	SHIP SPD KT	BURNG TIME SEC	CHARGE KG	CORRECTED SHOT TIME D H M S
1	E01	2736.00	12713.27	1.750	26190144.760	7.400	323.000	500.000	26 19 1 43.87
2	E02	2723.34	12704.33	1.570	26191506.780	6.200	73.000	50.000	26 19 15 6.55
3	E03	2726.31	12702.00	1.420	26194241.680	6.200	327.000	500.000	26 19 42 40.92
4	E04	2717.00	12651.17	1.750	27 85052.930	6.300	169.000	300.000	27 8 50 52.49
5	E05	2712.09	12645.67	1.774	27101625.920	6.000	176.000	125.000	27 10 16 25.49
6	E06	2707.29	12640.00	1.849	27115132.330	6.000	182.000	100.000	27 11 51 32.38
7	E07	2702.45	12634.47	1.851	27132133.570	6.700	175.000	125.000	27 13 21 33.10
8	E08	2653.00	12629.01	1.806	27144039.400	6.500	168.000	300.000	27 14 40 38.95
9	E09	2648.29	12618.00	1.817	27170635.970	6.900	326.000	500.000	27 17 6 35.13
10	E10	2646.36	12615.73	1.848	27181532.280	8.500	73.000	50.000	27 18 15 31.99
11	E11	2639.00	12607.00	1.923	27193509.230	6.200	332.000	500.000	27 19 35 8.46
12	E12	2650.23	12620.20	1.808	28 71826.350	7.900	105.000	22.500	28 7 18 26.46
13	E13	2652.17	12622.40	1.779	28 73423.390	8.200	86.000	22.500	28 7 34 23.06
14	E14	2653.15	12623.51	1.773	28 74151.160	8.000	73.000	10.000	28 7 41 50.37
15	E15	2654.12	12624.61	1.767	28 74925.620	8.000	76.000	10.000	28 7 49 25.34
16	E16	2655.09	12625.71	1.805	28 75805.730	8.000	76.000	10.000	28 7 53 5.45
17	E17	2656.06	12626.81	1.810	28 80544.120	7.800	75.000	10.000	28 8 5 43.84
18	E18	2657.03	12627.91	1.799	28 81417.620	8.000	79.000	10.000	28 8 14 17.32
19	E19	2658.89	12630.10	1.841	28 83015.960	7.600	83.000	5.000	28 8 30 15.66
20	E20	2659.78	12631.19	1.855	28 83745.360	8.100	82.000	5.000	28 8 37 45.55
21	E21	2700.67	12632.29	1.855	28 84544.540	8.000	83.000	5.000	28 8 45 44.23
22	E22	2701.56	12633.38	1.853	28 85314.790	7.900	80.000	5.000	28 8 53 14.49
23	E23	2703.42	12635.58	1.860	28 90946.220	8.000	83.000	2.000	28 9 9 45.91
24	E24	2704.39	12636.68	1.857	28 91813.620	7.900	83.000	2.000	28 9 18 13.31
25	E25	2705.35	12637.79	1.852	28 92640.620	7.900	81.000	2.000	28 9 26 40.32
26	E26	2706.32	12638.89	1.840	28 93513.820	8.200	82.000	2.000	28 9 35 13.51
27	E27	2708.25	12641.13	1.848	28 95245.390	8.000	85.000	2.000	28 9 52 45.07
28	E28	2709.21	12642.27	1.831	28100113.530	8.000	80.000	2.000	28 10 1 13.23
29	E29	2710.17	12643.40	1.817	28101010.720	8.000	79.000	2.000	28 10 10 10.42
30	E30	2711.13	12644.54	1.807	28101911.780	8.300	82.000	2.000	28 10 19 11.46
31	E31	2713.07	12646.77	1.790	28104509.920	8.500	82.000	5.000	28 10 45 9.60
32	E32	2714.05	12647.87	1.776	28105439.680	8.000	84.000	5.000	28 10 54 39.37
33	E33	2715.04	12648.97	1.777	28110409.150	8.300	81.000	5.000	28 11 4 8.84
34	E34	2716.02	12650.07	1.718	28111345.390	8.900	83.000	5.000	28 11 13 45.05
35	E35	2717.93	12652.25	1.570	28112938.380	8.900	75.000	10.000	28 11 29 38.08
36	E36	2718.86	12653.34	1.449	28113830.270	8.800	76.000	10.000	28 11 38 29.97
37	E37	2719.79	12654.42	1.431	28114626.060	8.700	73.000	10.000	28 11 46 25.77
38	E38	2720.72	12655.50	1.442	28115503.860	9.000	75.000	10.000	28 11 55 3.55
39	E39	2721.66	12656.59	1.396	28120333.940	9.000	74.000	10.000	28 12 3 33.64
40	E40	2722.59	12657.67	1.452	28121216.940	9.000	94.000	22.500	28 12 12 16.56

Appendix Table 2.

LINE A

SHOT NO.	NAME	LAT D M N	LON D M E	DEPTH KM	DAY SHOT TIME1 D H M S	SHIP SPD KT	BURNG TIME SEC	CHARGE KG	CORRECTED SHOT TIME D H M S
1	E42	2739.58	12724.36	1.679	29 75407.570	8.100	70.000	50.000	29 7 54 7.31
2	E43	2737.88	12718.81	1.659	29 83001.270	7.900	70.000	50.000	29 8 30 1.01
3	E44	2736.18	12713.25	1.535	29 90328.550	8.100	188.000	100.000	29 9 3 27.96
4	E45	2734.95	12707.42	1.517	29100927.800	8.000	187.000	100.000	29 10 9 27.22
5	E46	2733.71	12701.59	1.624	29111130.310	8.000	69.000	50.000	29 11 11 30.05
6	E47	2732.48	12655.75	1.562	29114358.720	8.100	71.000	50.000	29 11 43 58.45
7	E48	2731.24	12649.92	1.625	29121715.690	8.500	165.000	100.000	29 12 17 15.14
8	E49	2730.01	12644.09	1.537	29134226.470	8.400	184.000	100.000	29 13 42 25.87
9	E50	2730.32	12645.55	1.553	29143912.040	6.500	83.000	2.000	29 14 39 11.77
10	E51	2730.63	12647.01	1.580	29144950.290	7.400	82.000	2.000	29 14 49 50.00
11	E52	2730.94	12648.46	1.626	29150004.930	6.800	81.000	2.000	29 15 0 4.66
12	E53	2731.55	12651.38	1.615	29152223.380	7.200	82.000	5.000	29 15 22 23.09
13	E54	2731.86	12652.84	1.596	29153327.530	6.400	82.000	5.000	29 15 33 27.27
14	E55	2732.17	12654.30	1.597	29154418.590	6.000	86.000	5.000	29 15 44 18.32
15	E56	2732.79	12657.21	1.540	29160602.250	7.400	72.000	20.000	29 16 6 1.99
16	E57	2733.10	12658.67	1.537	29161652.590	6.800	75.000	20.000	29 16 16 52.34
17	E58	2733.40	12700.13	1.598	29162809.850	7.100	73.000	20.000	29 16 28 9.60
18	E59	2734.02	12703.04	1.667	29164943.050	6.800	82.000	5.000	29 16 49 42.77
19	E60	2734.33	12704.50	1.661	29170150.150	6.300	81.000	5.000	29 17 1 49.89
20	E61	2734.64	12705.96	1.567	29171244.510	6.500	82.000	5.000	29 17 12 44.24
21	E62	2735.25	12708.88	1.528	29173520.310	6.400	81.000	2.000	29 17 35 20.05
22	E63	2735.56	12710.33	1.405	29174617.830	6.700	74.000	2.000	29 17 46 17.53
23	E64	2735.87	12711.79	1.392	29175714.390	7.000	80.000	2.000	29 17 57 14.12

DELP 1984年度中部沖縄トラフ研究航海報告

II. 地震構造探査

南雲昭三郎[1]・木下　肇[2]・笠原順三[1]・大内　徹[3]
徳山英一[4]・浅沼俊夫[2]・是澤定之[1]・秋吉日奈子[2]

1) 東京大学地震研究所
2) 千葉大学理学部
3) 神戸大学理学部
4) 東京大学海洋研究所

A. 多成分反射法による堆積構造探査

堆積構造を調べる目的をもって，多成分反射法地震探査を三測線おこなった（図 II-1）．測線は沖縄トラフ中部域の北東—南西方向に伸びる細長いトラフ軸域を直交するように設けた．特に測線 2 は，異常に高い熱流量が知られた Iheya Deep の近傍を通っている（図 II-1）．記録断面を図 II の 2～5 に，そのラインスケッチを図 II の 6～9 に示す．連続した厚い堆積層 A，B は島尻層群 (late Miocen～early Pleistocene) に対比される．測線の 2 の Iheya Deep には基盤岩層のもり上がりがみえているようである．表 II-3 は堆積構造の特徴をまとめたものである．測線 2 のリフト中央部には，マグマ溜りからの反射波と思われる位相がみられる．

B. 海底地震計エアガンによる精密地殻構造探査

地殻浅部の微細構造を調べる目的をもって，海底地震計と大容量エアガンによる屈折法地震探査を行った．屈折法測線 A，B（図 II-14）の内，地震計 No. 2 と 3 の間，No. 4 と 6 の間において大容量エアガン（20 リットル）の爆発を行なった．測線 A，B の海底地形断面は図 II の 15，16 に示す．大容量の仕様は表 II-5 に示す通りである．記録断面の一例を図 II-17 に示す．水平構造仮定の下に求められた各観測点下の構造（暫定的）を図 II-18 に示す．

C. 火薬による屈折法地震探査

沖縄トラフ中部域において，海洋地殻がすでに生成されているかどうか，もし，生成されていないとすれば，大陸地殻がどれくらい壊れているかを調べる目的をもって，火薬を用いた屈折法地震探査を行なった．

測線は 2 本，測線 A はリフト軸の真上付近に設け，測線 B は中部域の平均的軸上に設けた（図 II-19）．海底地震計は測線上に 4 台，測線 B 上に 4 台設置した．火薬爆発点と海底地震計との配置は図 II-20 の通り．火薬爆発回数 64 回（最大薬量 500 kg），消費火薬総量 4 t．海底地震計は自然地震観測用も含めて，音響切り離し方式自己浮上型（ERI-AR81 型）10 台と最近開発したデジタル式海底地震計 1 台　計 11 台を用いた．デジタル式海底地震計は屈折法探査終了後に回収した．残りの地震計は引続き自然地震観測を行ない，約 2 ヶ月後淡青丸（海洋研究所）の航海において全部回収した．発破点の位置精度は，オンラインの航跡表示システムを用いた航法により，予定点の 0.1 海里以内におさめることができた．

（結果） 測線 A は，地形および地磁気異常から推定されたリフト軸上に設けられたものであったが，カコウ岩質層と思われる 6.0 km/sec 層が厚く現われており，未だ海洋性地殻が生成されていないことが判明した．測線 B においては，6 km/sec 層の下に 6.8 km/sec 層（下部地殻）があり，その屈折波は減衰が大きいことが判明した．またモホ不連続面からの屈折波は震央距離 130 km 以遠でも検出されなかった．恐らくトラフ軸下の上部マントルは異常であって，地震波速度と減衰 Q と共に低いものと思われる．この異常は恐らく力学的破壊のみならず，熱的非弾性，部分熔融などに由来しているのであろう．6.0 km/sec 層の上は P 波速度約 4 km/sec の薄層で覆われている．周辺の地質構造から，この地層は白亜紀堆積物と推定される．おおよその構造を図 II-26 に示す．

以上のことから沖縄トラフ中部域では，大陸性地殻が未だ残っているがその破壊は下部地殻にまで及んでおり，上部マントルは P 波速度および減衰 Q 共に異常に低いといえよう．

D. 微小地震活動

10 観測点において（図 II-19）約1ヶ月間の連続観測を行なった（1984年8月26日から9月26日まで）．従来この海域の微小地震活動は陸（島）からの観測網では検出されていなかったが，今回の観測によって活発な微小地震活動がほとんど中部域全域にわたって起こっていることが判明した．比較的大きな地震を含む群発地震活動が3ヶ所（図 II-27 参照）起こっていた．自然地震の記録において，P，S相以外に，マグマ・シートからの反射波と思われるよう顕著な相が表われたものがあった（図 II-28, 29）．

自然地震の P 波の減衰も震央距離 120 km を起えると著しい．これは人工震源にみられたものと同じような性質である．火山性微動に似た震動が2種類記録された．1つは絶間なく起こる孤立型ショックの系列（図 II-32）であり，もう1つは正弦波的震動（卓越周波数 5—7 Hz）（図 II-33）である．これらの自然地震活動の示す特徴は，屈折法構造探査の結果と相俟って中部沖縄トラフ海域は incipient spreading（海洋性地殻生成の発端）の時期に当たっており，大陸性地殻の破壊がマグマ活動を伴って，下部地殻まで及んでいることを示していると思われる．